Deformation Mechanisms

A brief synopsis

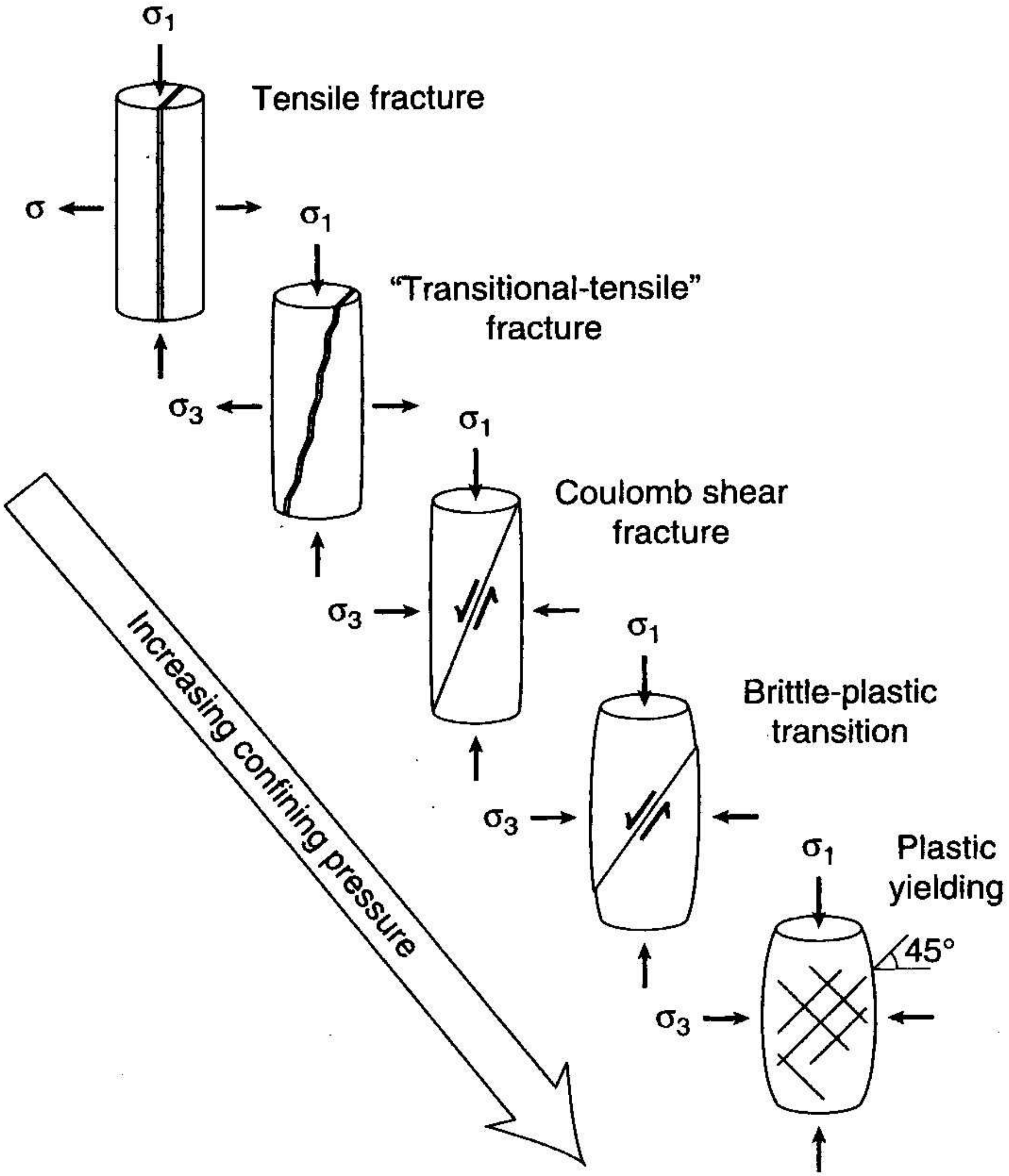
σ_1
Tensile fracture
σ
σ_1
"Transitional-tensile" fracture
σ_3
σ_1
Coulomb shear fracture
σ_3
σ_1
Brittle-plastic transition
σ_3
σ_1
Plastic yielding
45°
σ_3
Increasing confining pressure

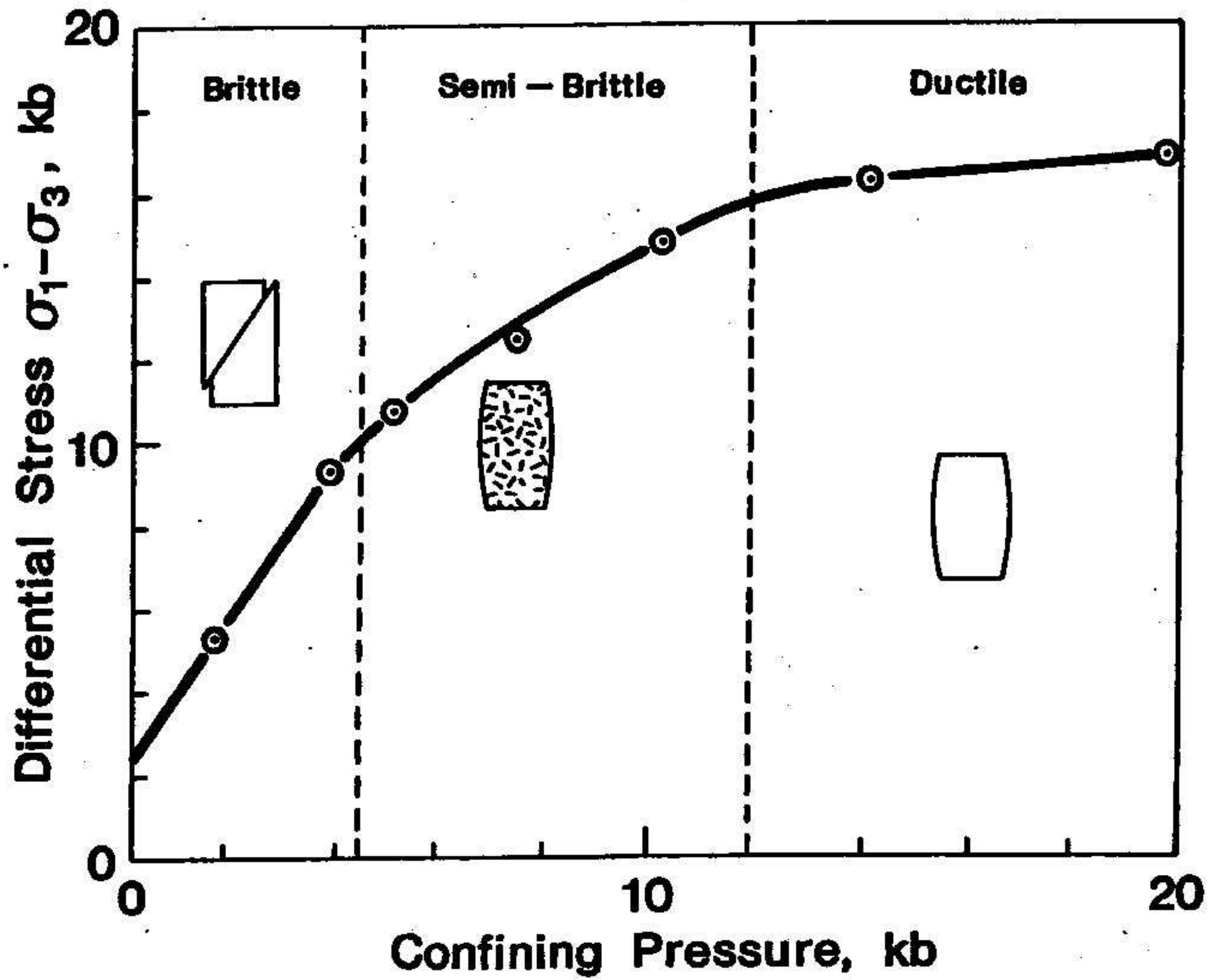

Figure 6-10 Brittle-to-ductile transition of pyroxenite. Effect of confining pressure on the strength of Sleaford Bay clinopyroxenite tested in triaxial compression. *(After Kirby, 1980.)*

CONTINENTAL CRUST

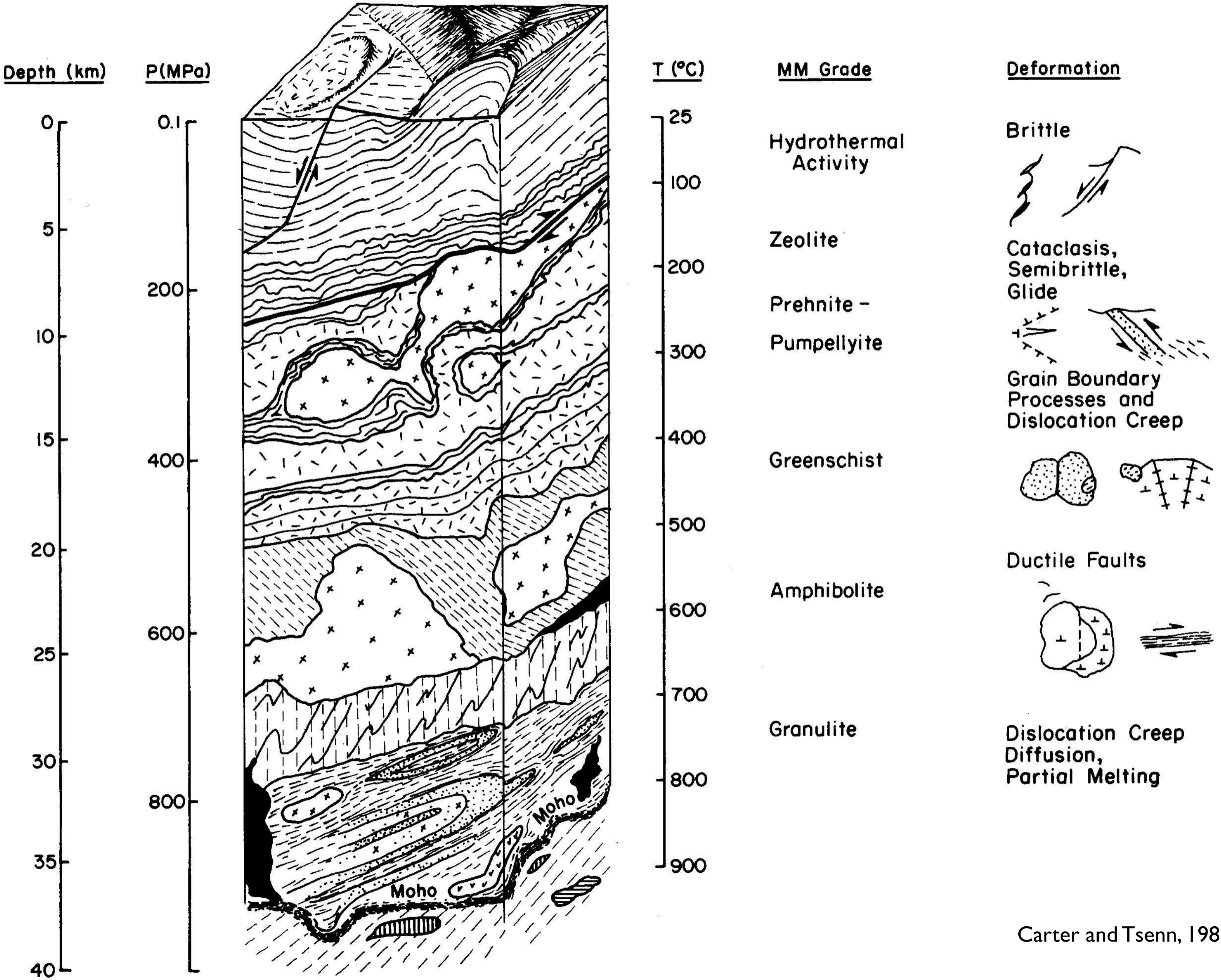

Carter and Tsenn, 1987

Seismo-structural section through the San Andreas fault

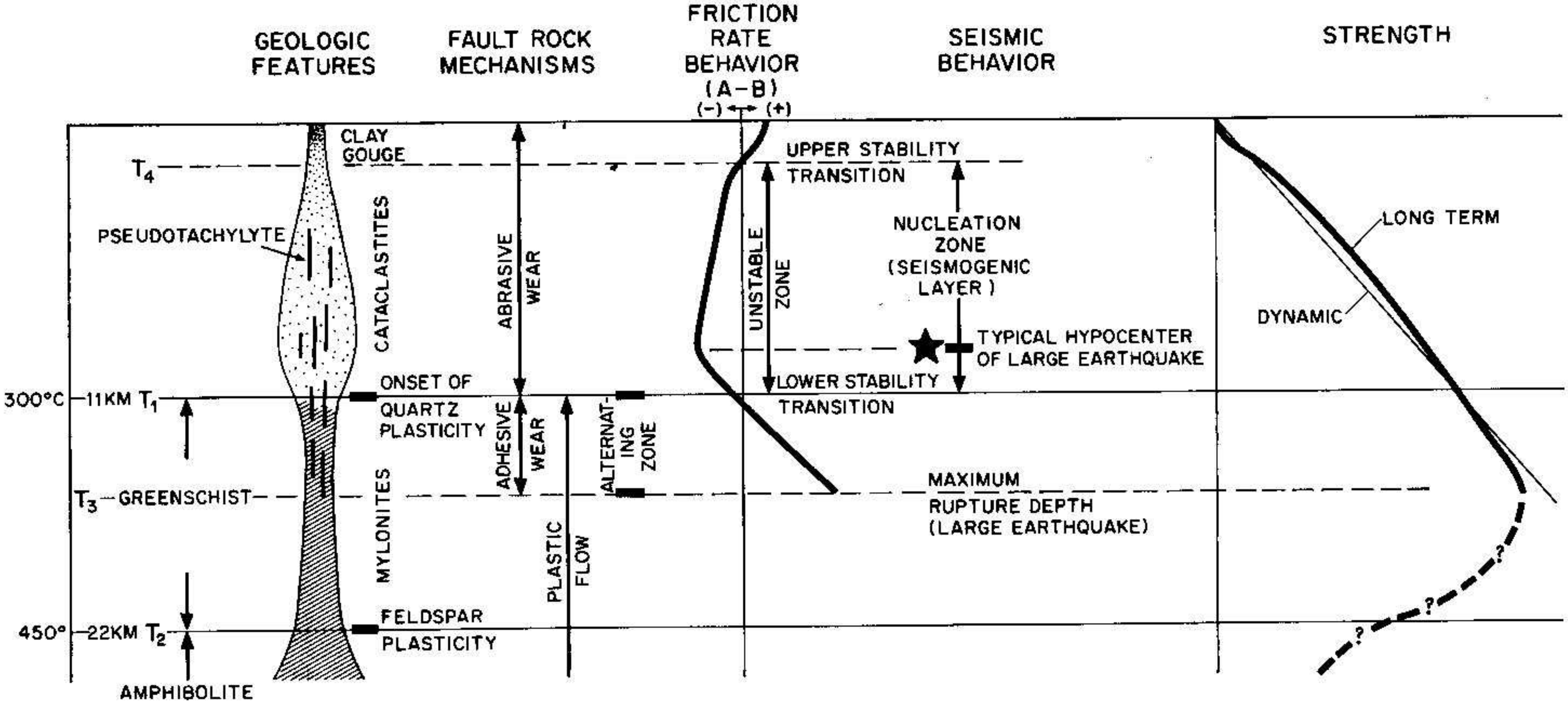

Scholtz, 1988

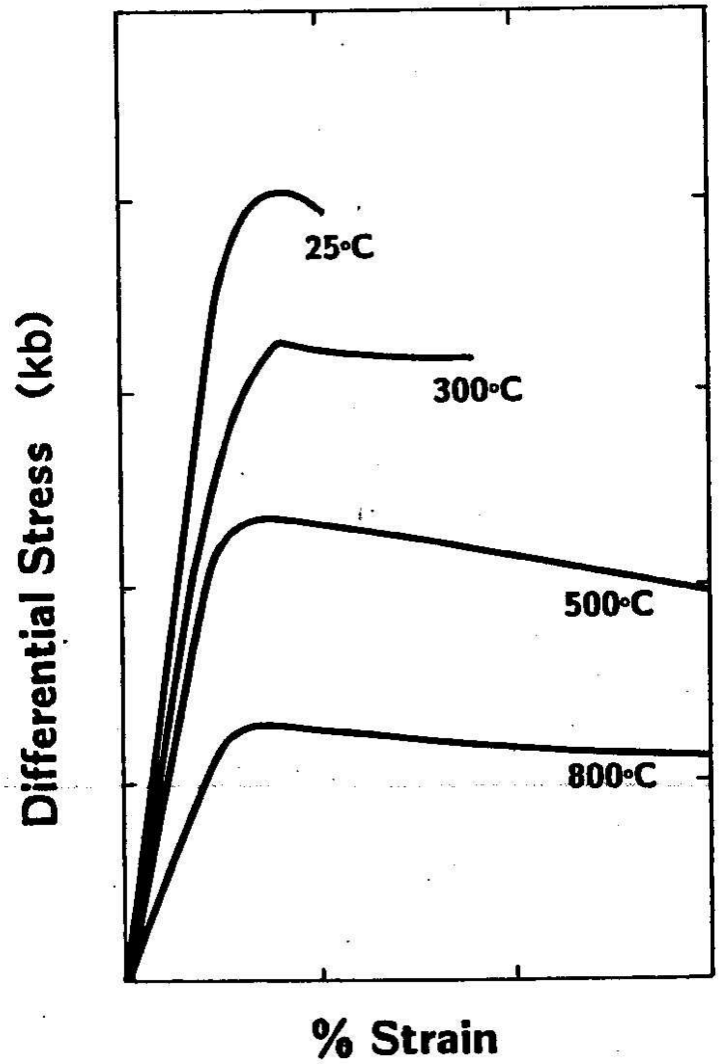

Figure 6-11 Temperature effects on the behavior of granite tested in compression. *(After Heard, 1960.)*

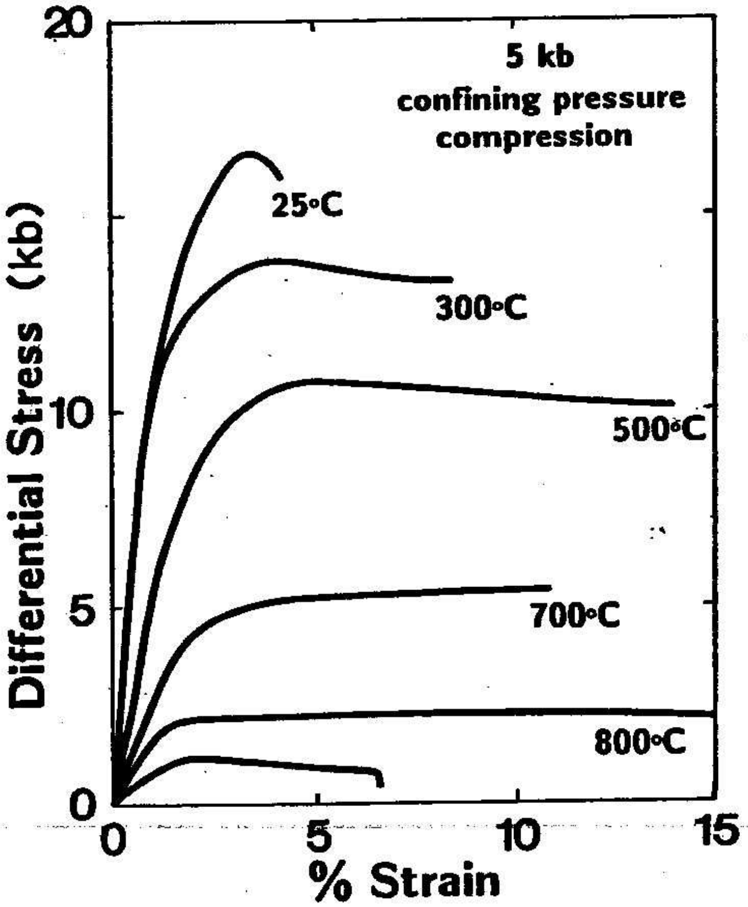

Figure 6-12 Temperature effects on the behavior of basalt tested in compression. *(After Heard, 1960.)*

Low-Temperature Crystal Plasticity

Processes that depend more on differential stress than on temperature, and that change a mineral's shape without melting, fracturing or faulting.

- Pressure solution
- Kinking
- Dislocation glide
- Mechanical twinning

Low-Temperature Crystal Plasticity

Processes that depend more on differential stress than on temperature, and that change a mineral's shape without melting, fracturing or faulting.

- Pressure solution

Pressure solution

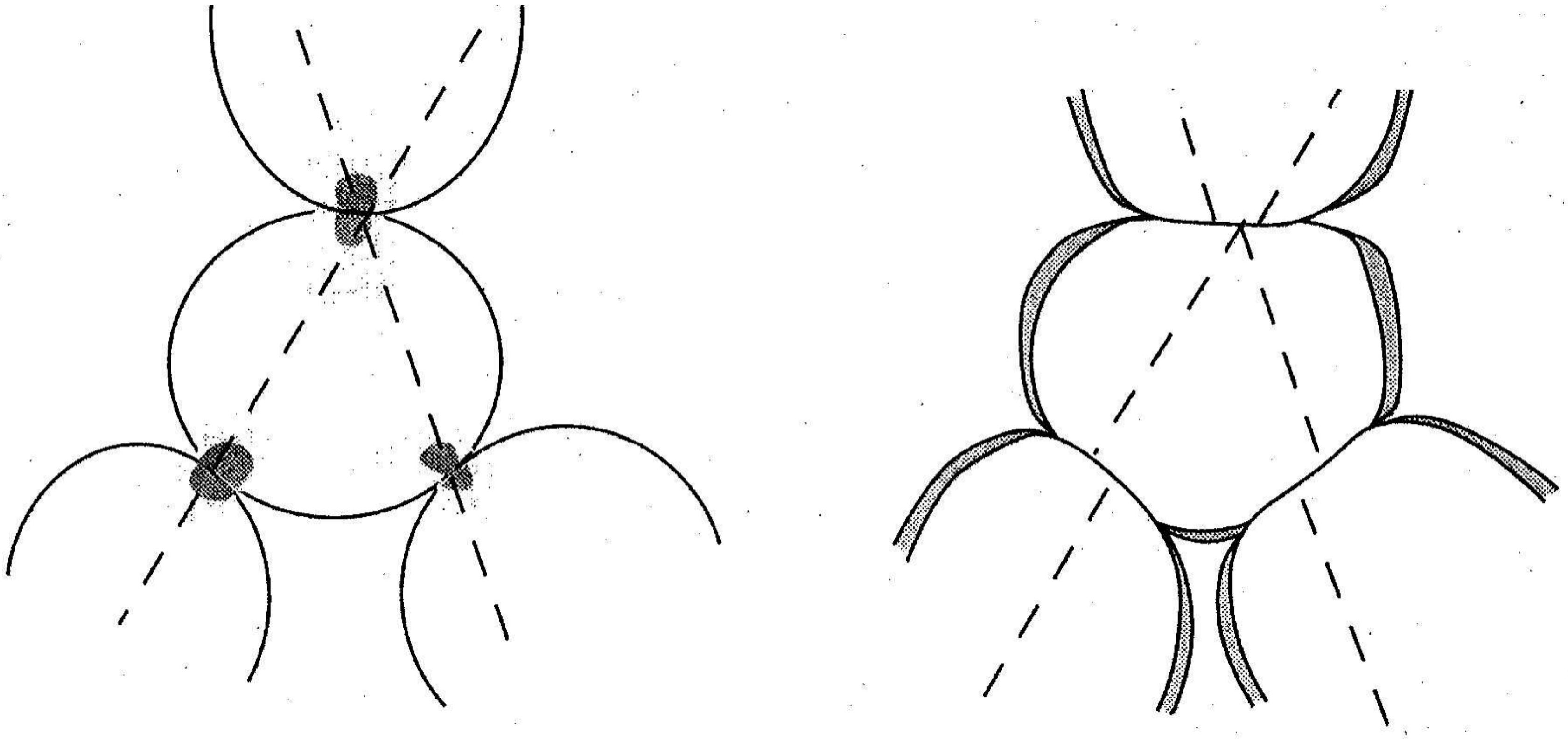

Low-Temperature Crystal Plasticity

Processes that depend more on differential stress than on temperature, and that change a mineral's shape without melting, fracturing or faulting.

- Pressure solution
- Kinking

Development of kink bands

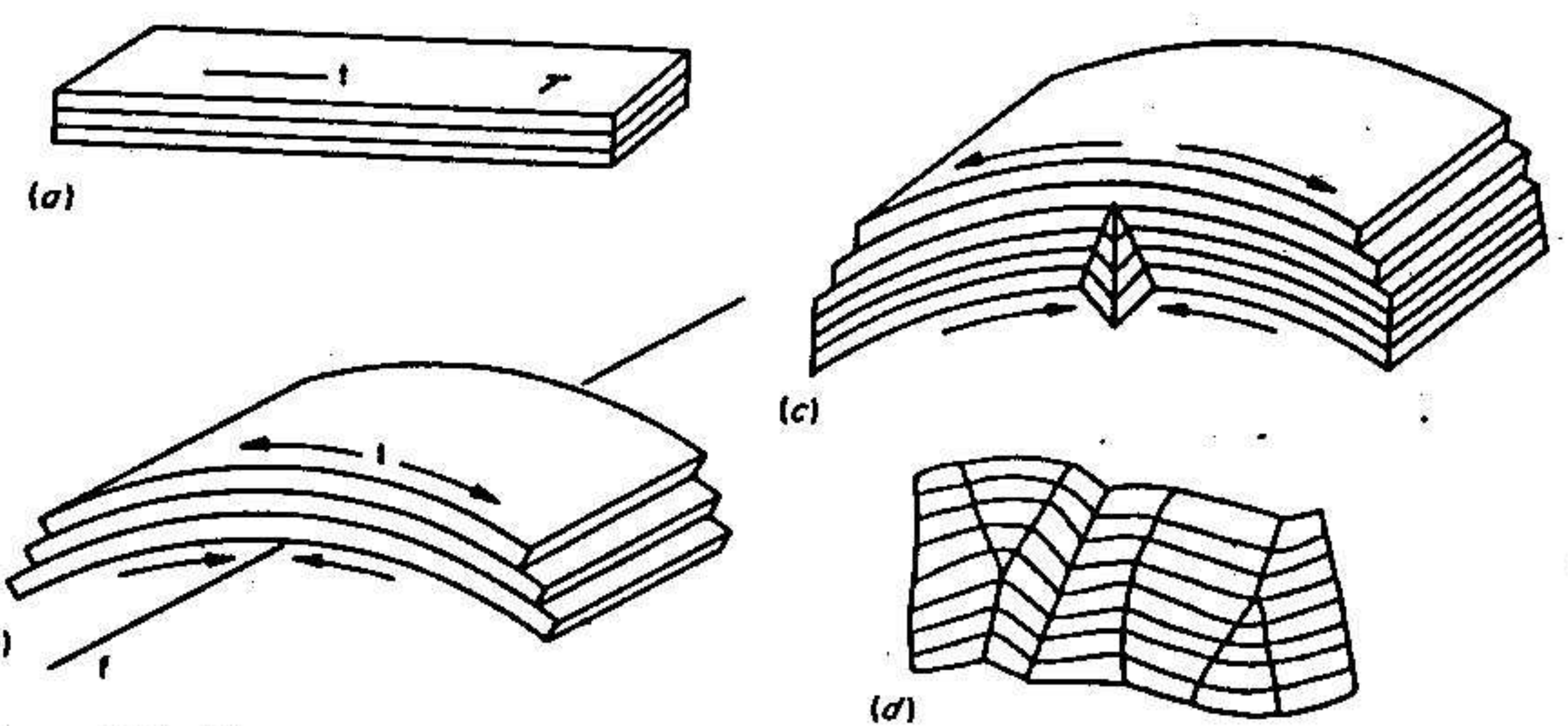

Figure 7-7 Sketch showing the development of kink bands by the mechanism of bend gliding. (*a*) Undistorted crystal; (*b*) crystal bent by "two-sided" gliding parallel to the layer of atoms; (*c*) initial stage kinking leading to a chevron-shaped kink; (*d*) complex kinking as seen in a section normal to *f*. T = gliding plane, *t* = gliding line, *f* = axis of rotation or bending. (*After Mugge, 1898.*)

Development of kink bands

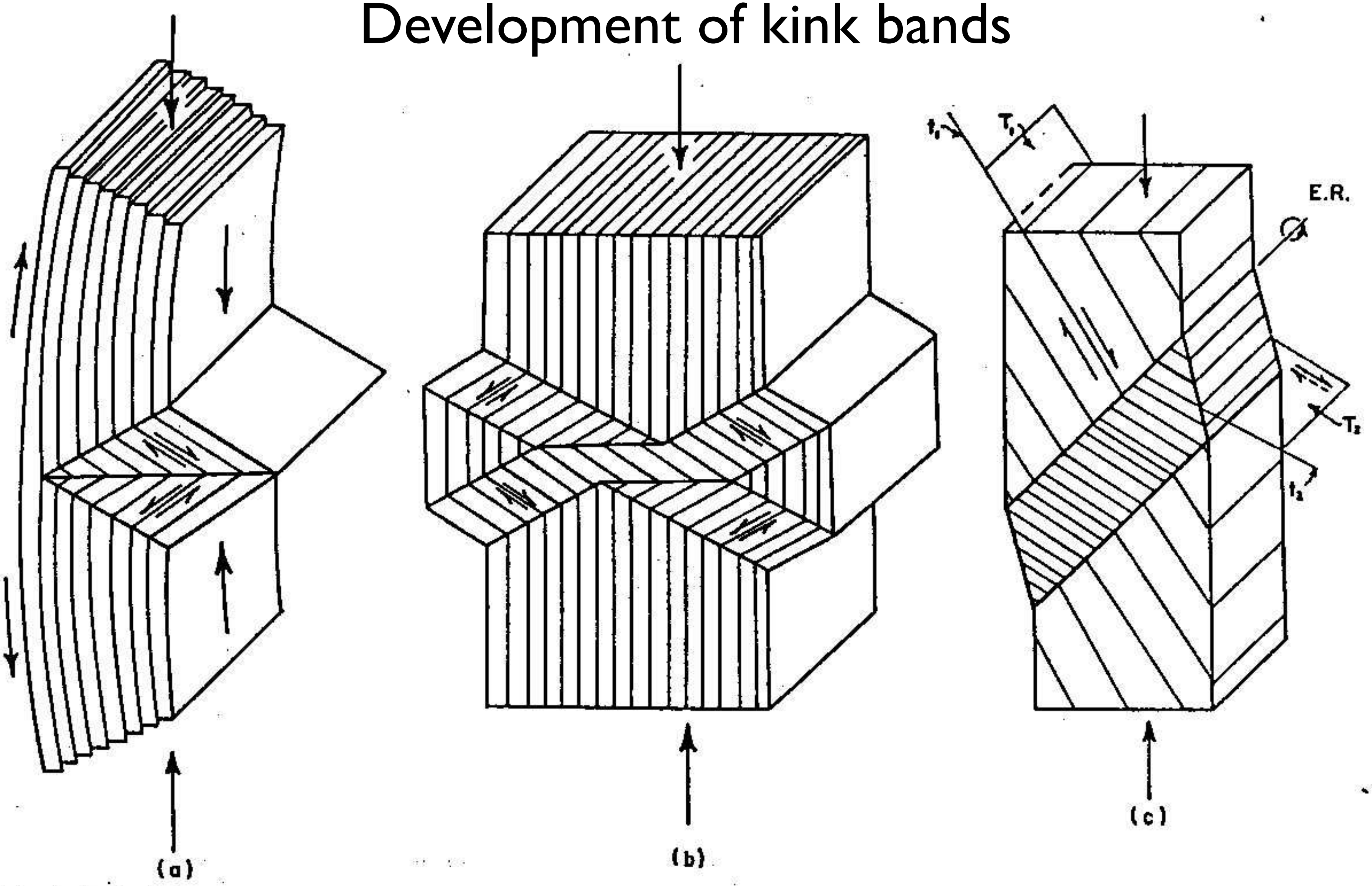

Figure 7-8 Schematic drawings of three types of kink bands in crystals. (*a*) Kink bands in crystals loaded parallel to strong planar anisotropy. (*b*) Intersecting conjugate kinks loaded parallel to a strong planar anisotropy. (*c*) Symmetrical kink in crystal whose slip plane T_1 is in an orientation of high shearing stress. (*From Carter and Raleigh, 1969.*)

Low-Temperature Crystal Plasticity

Processes that depend more on differential stress than on temperature, and that change a mineral's shape without melting, fracturing or faulting.

- Pressure solution
- Kinking
- Dislocation glide

Undeformed lattice

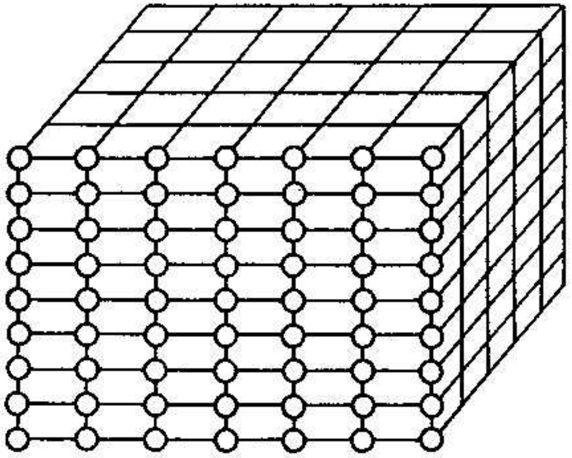

Dislocation glide

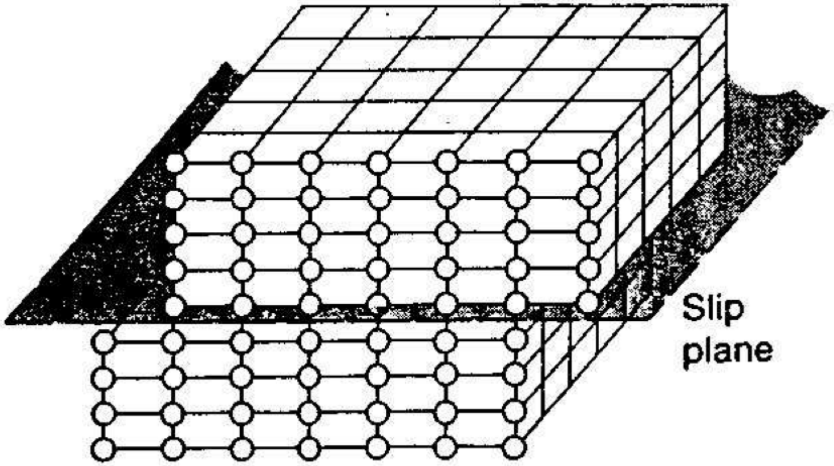

Low-Temperature Crystal Plasticity

Processes that depend more on differential stress than on temperature, and that change a mineral's shape without melting, fracturing or faulting.

- Pressure solution
- Kinking
- Dislocation glide
- Mechanical twinning

Mechanically twinned calcite lattice

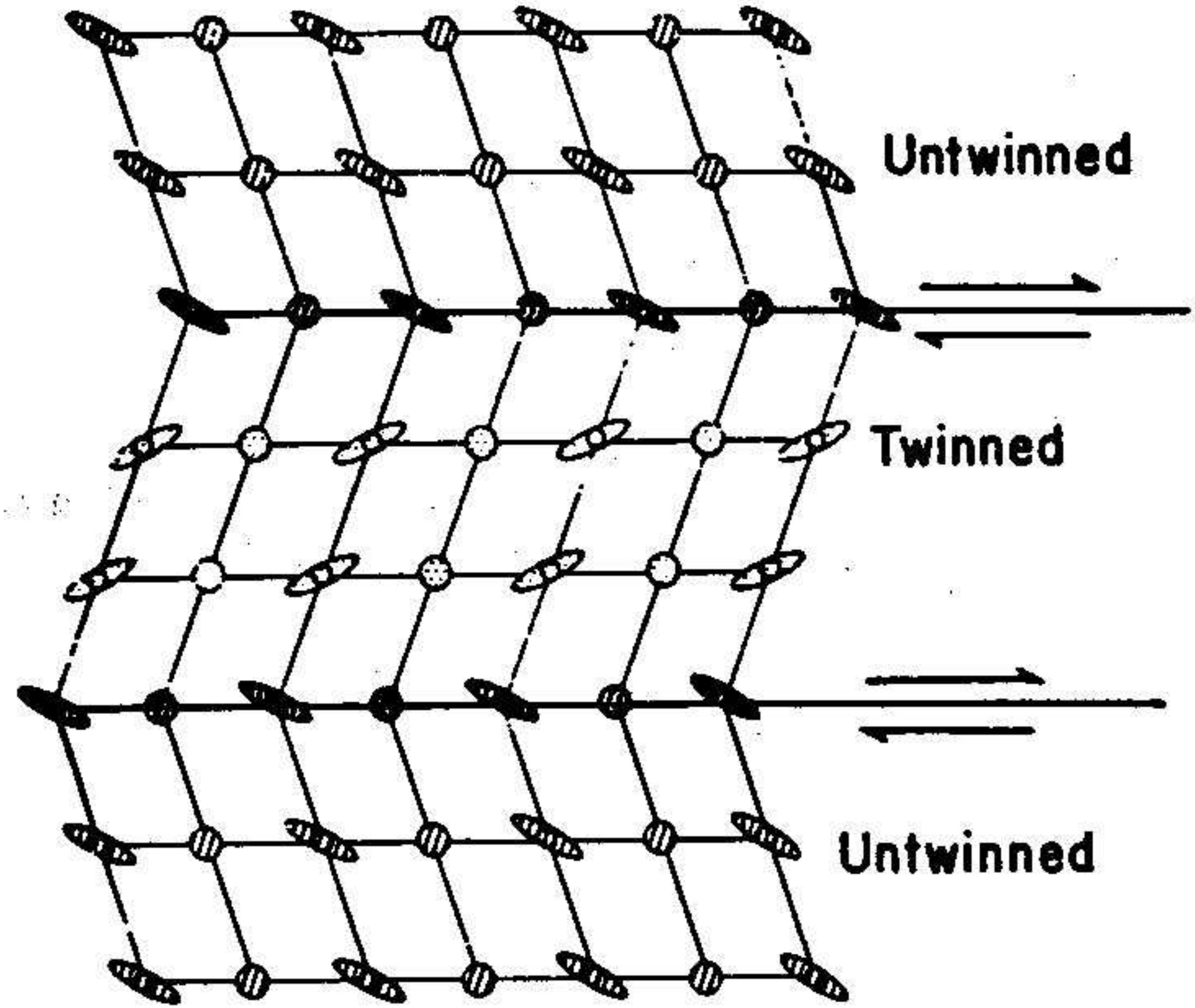

Mechanically twinned lattice

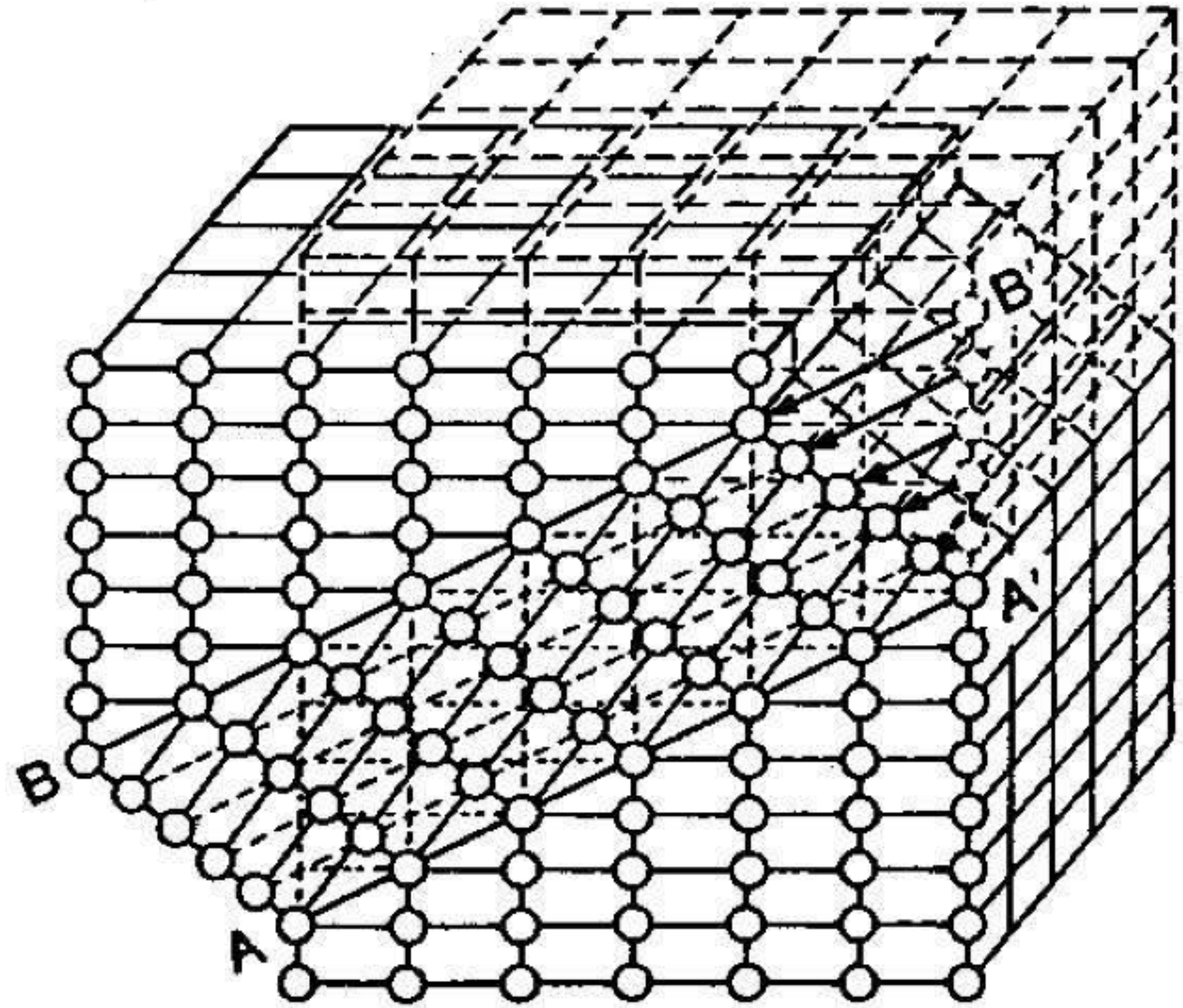

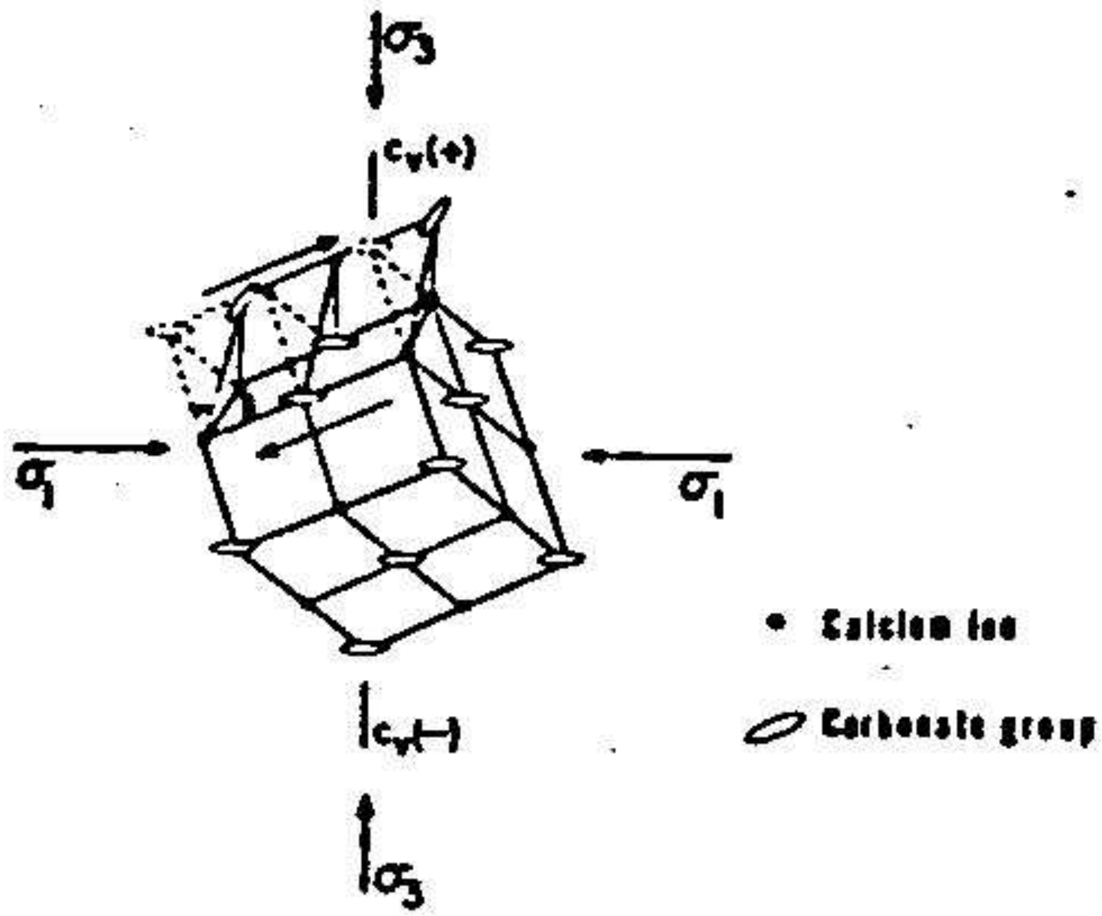

LOAD FAVORABLE FOR TWINNING

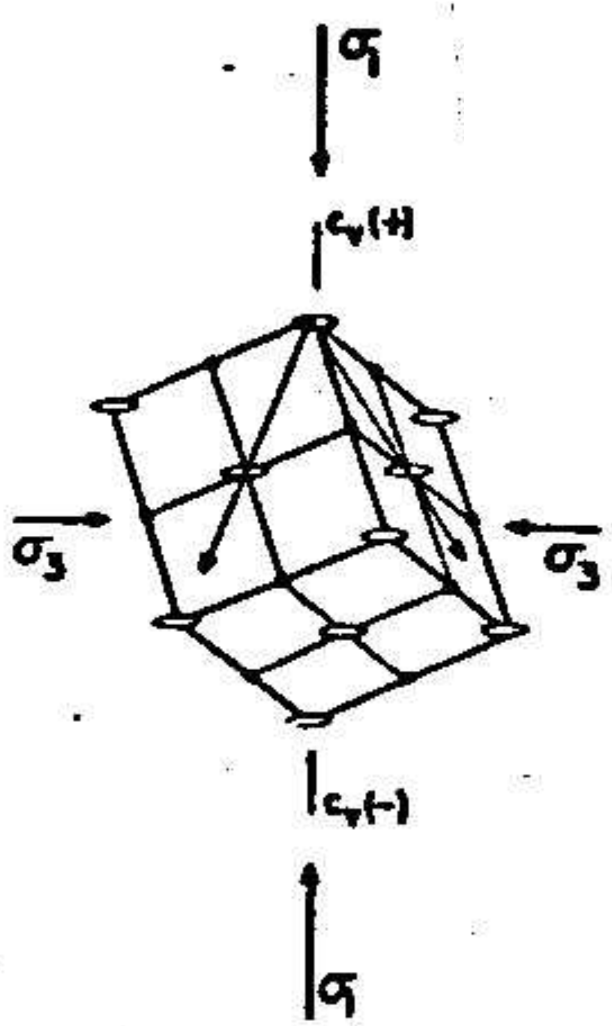

LOAD UNFAVORABLE FOR TWINNING
(FAVORABLE FOR TRANSLATION ON r AND f)

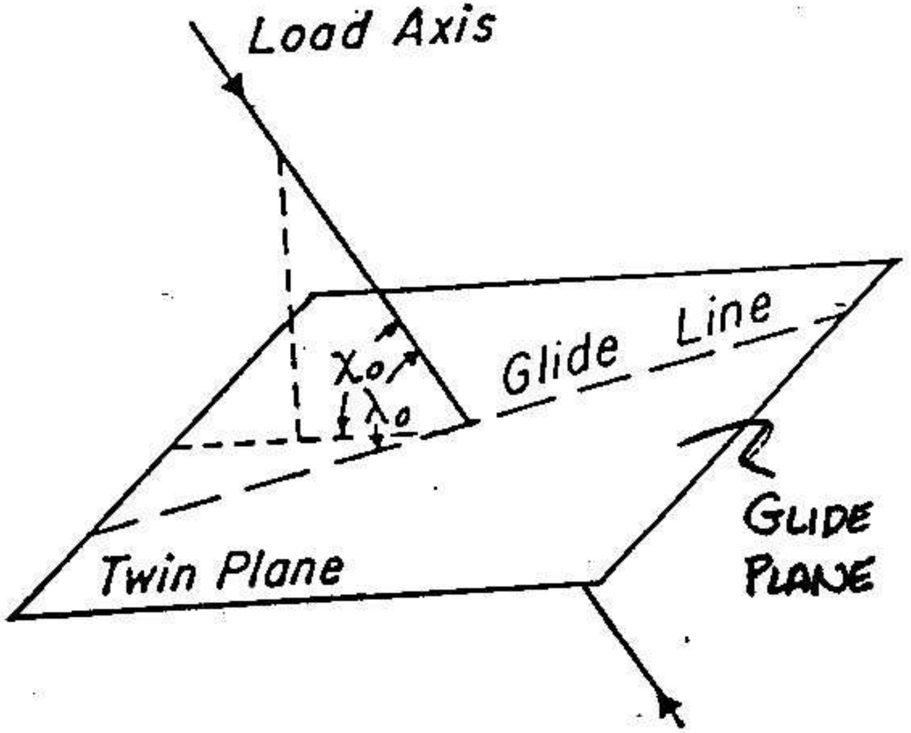

RESOLVED SHEAR STRESS COEFFICIENT S_o IS A FUNCTION OF THE ANGLES BETWEEN THE GLIDE PLANE AND THE LOAD AXES (χ_o) AND THE GLIDE LINE AND THE LOAD AXIS (λ_o).

$$S_o = \sin \chi_o \cos \lambda_o$$

$$\tau = S_o(\sigma_1 - \sigma_3) = \frac{\sigma_1 - \sigma_3}{2} \sin 2\theta$$

MAX τ OCCURS WHEN $\theta = 45°$

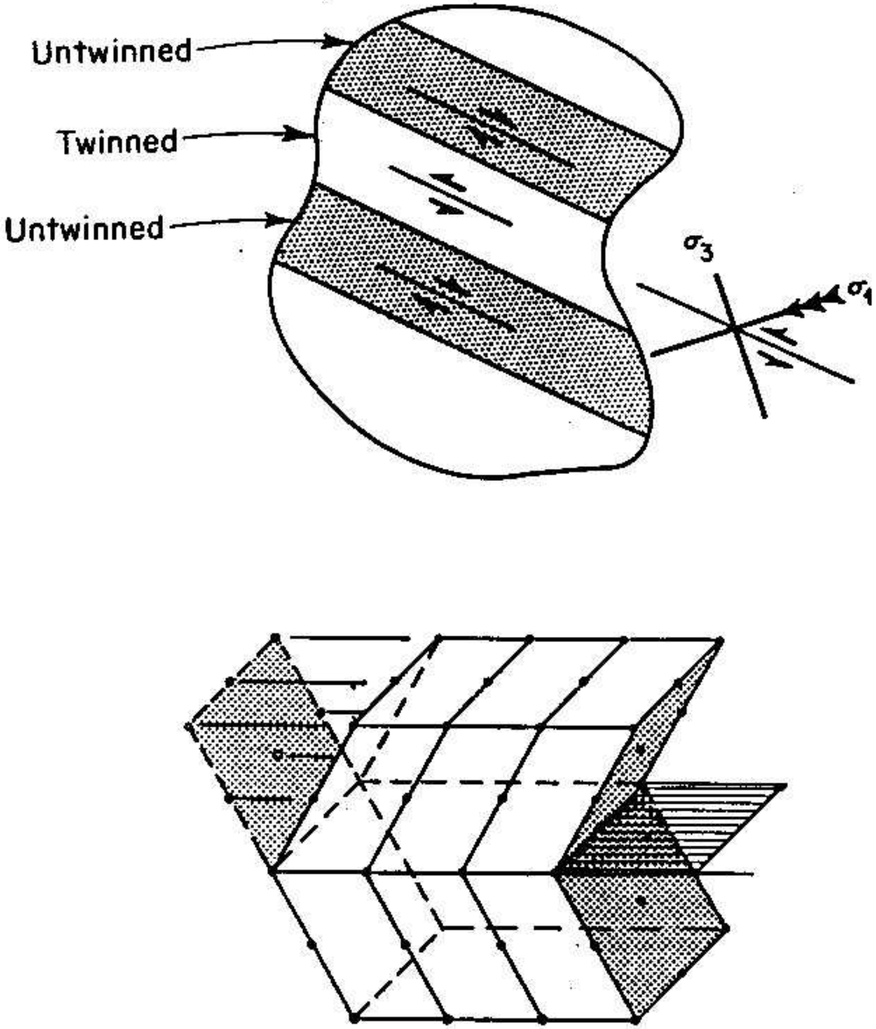

Figure 7-6 (*Top*) Twin gliding is most likely to occur when the principal stress direction is oriented at an angle that will produce high shear stress on the potential glide surface. (*Center*) A section through a twinned calcite crystal. (*After Friedman, 1963, Jour. of Geology, by permission of Univ. of Chicago.*) (*Bottom*) A block diagram showing displacements across a horizontal twin plane. (*After Carter and Raleigh, 1969.*)

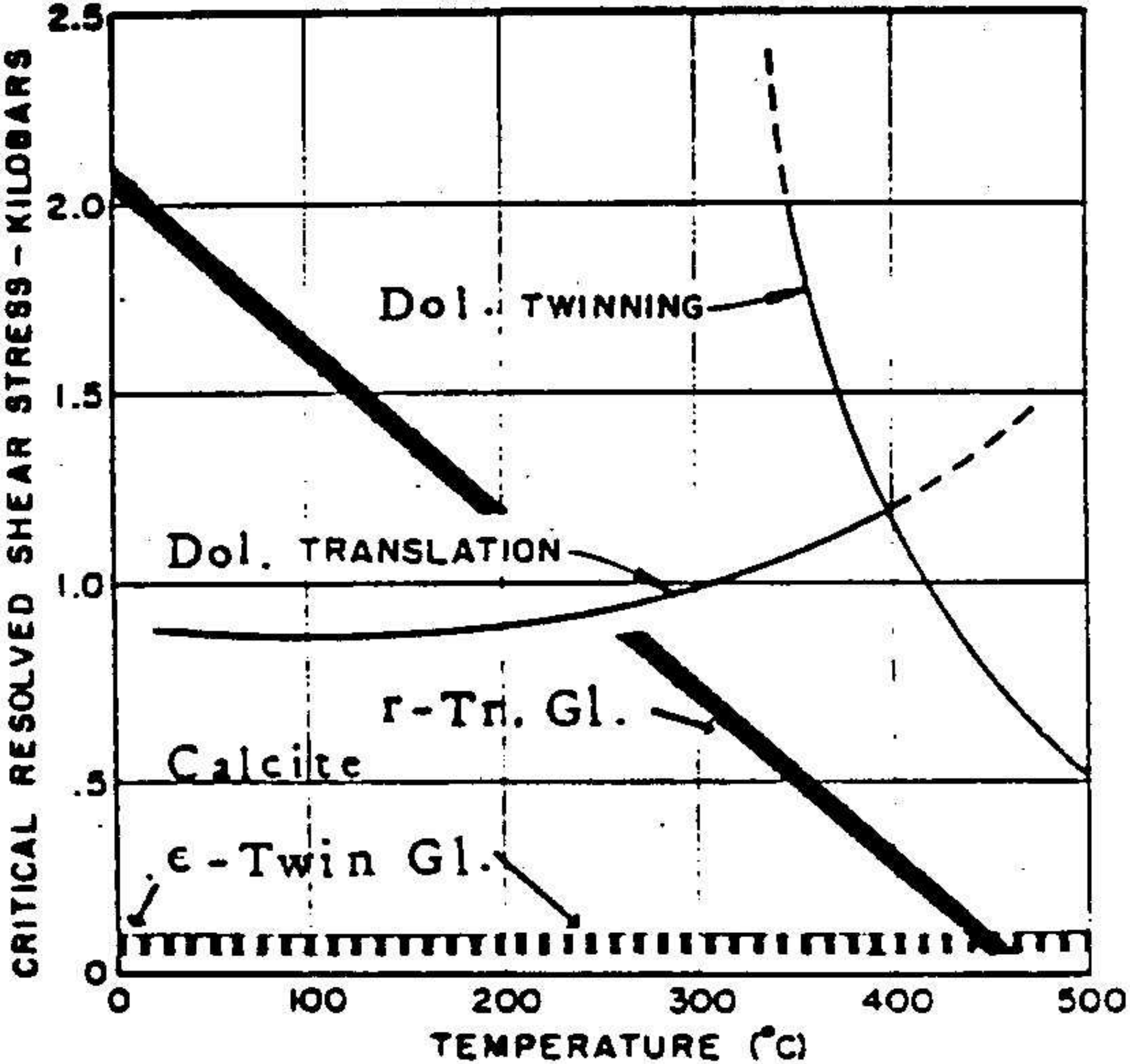

Figure 60. Critical resolved shear stress for dolomite (Dol.) and calcite (e and r) versus temperature.

High-Temperature Crystal Plasticity

Diffusion-assisted and hence temperature-dependant processes that change a mineral’s shape without melting, fracturing or faulting

Point defects: vacancies, interstitials, substitutions

Vacancies

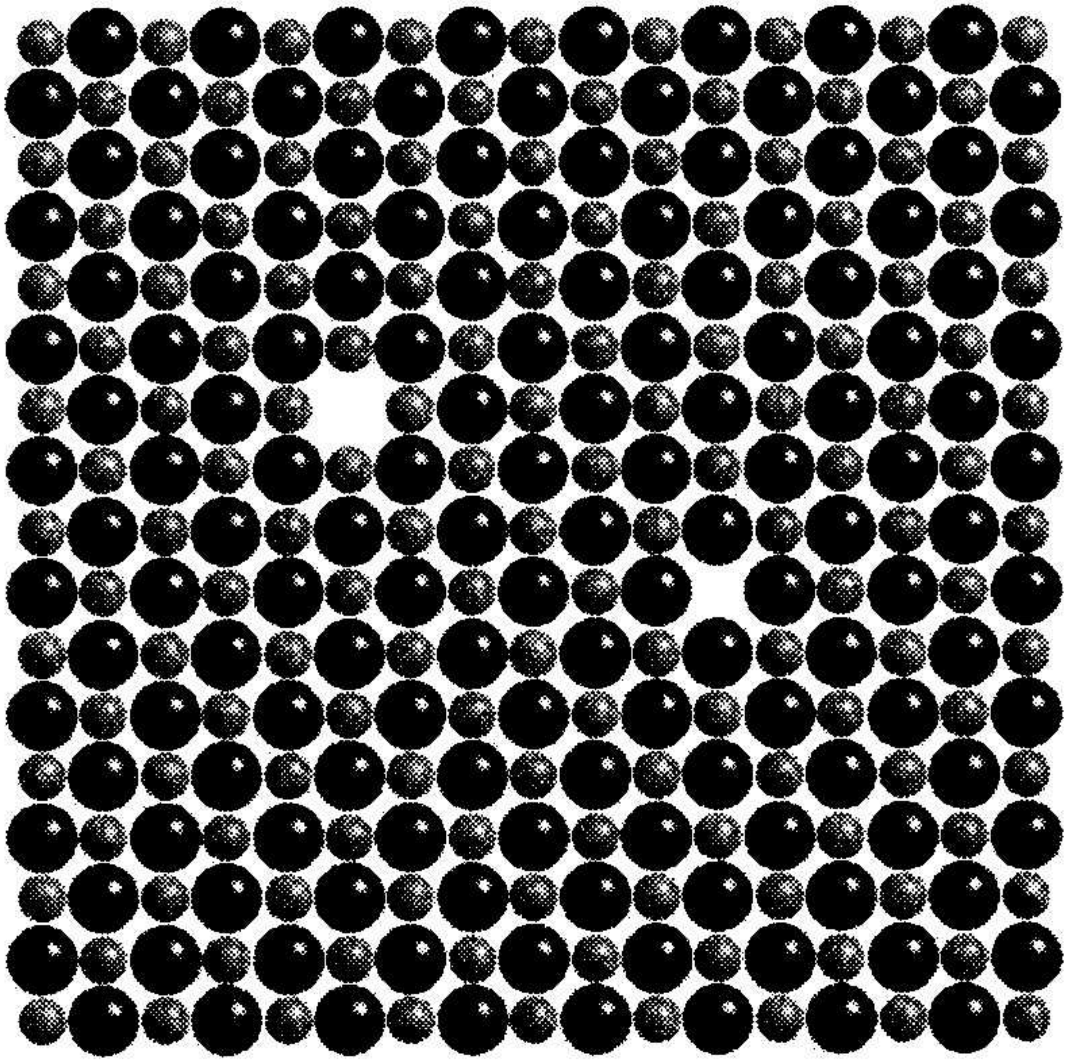

Fig. A.1 Cation and anion charge-balanced Shottky defects in NaCl.

Interstitial atoms

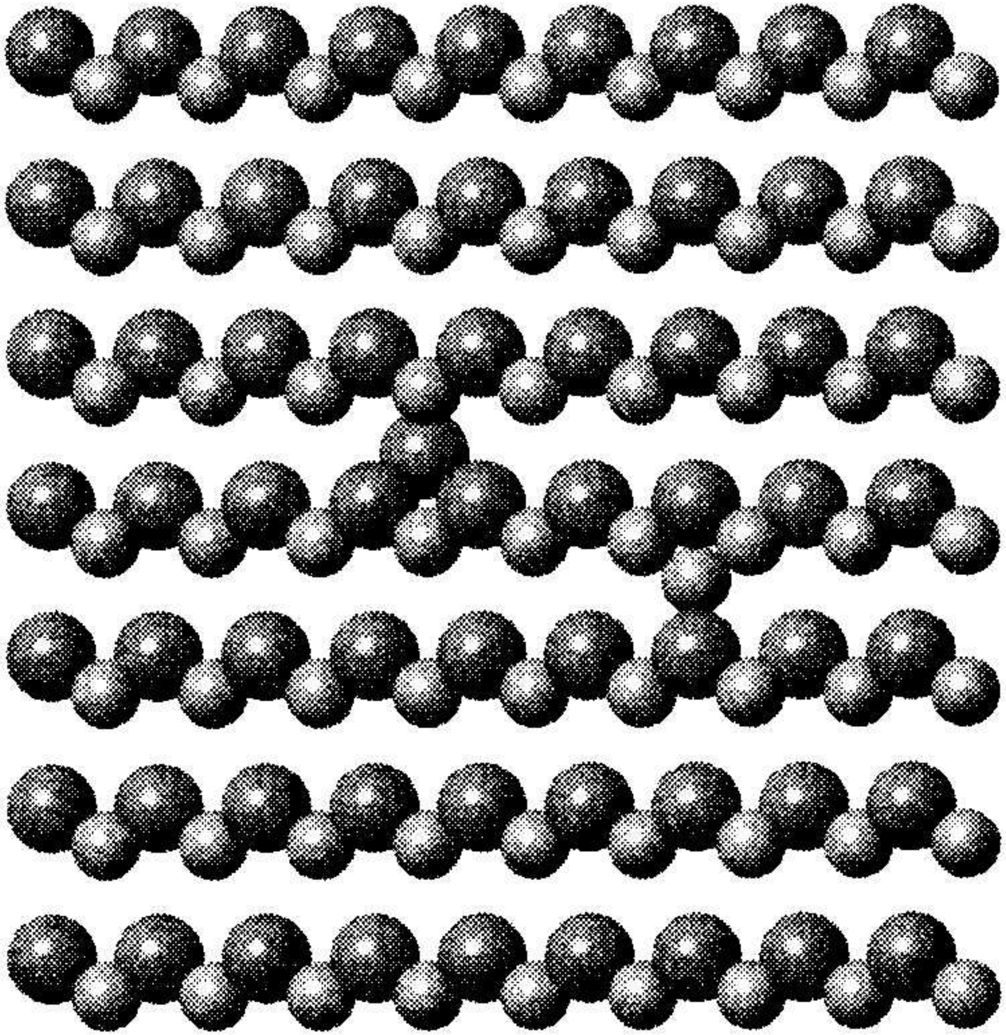

Fig. A.2 Pair of charge-balanced Frenkel defects in AgI.

Substitution errors

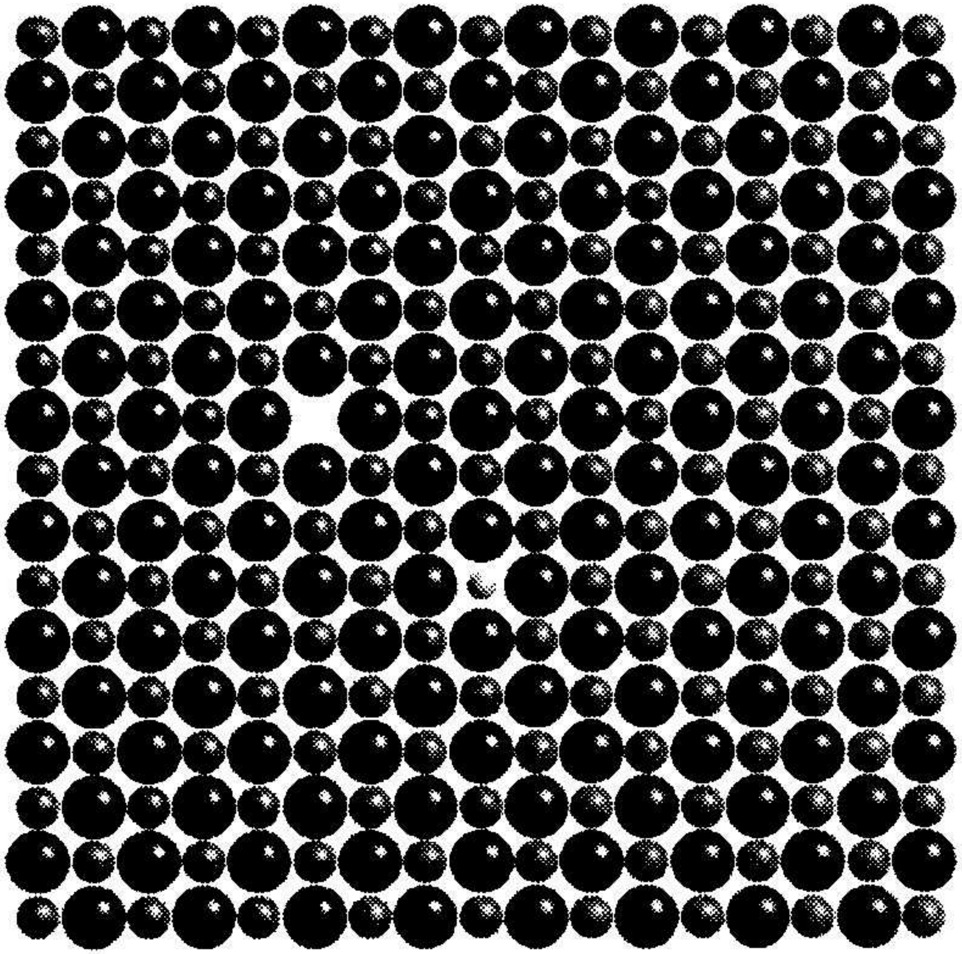

Fig. A.3 Substitution of a Ca^{2+} cation for a Na^{+} cation in NaCl, accompanied by the formation of a vacant cation site in order to maintain charge neutrality.

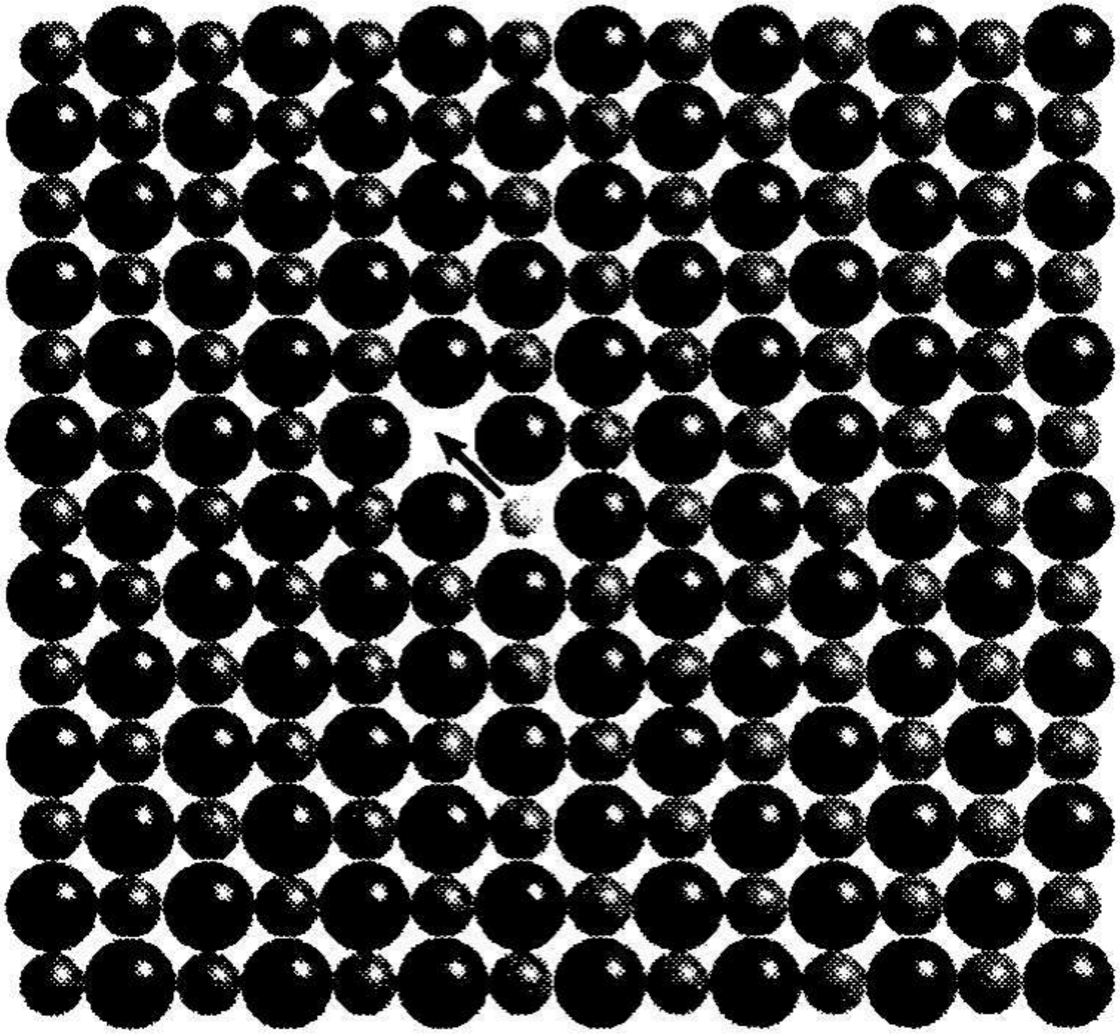

Fig. A.4 Diffusion of a cation in NaCl assisted through the presence of Shottky defects.

Line defects

- Twins
- Dislocations
  - Edge
  - Screw
  - Mixed

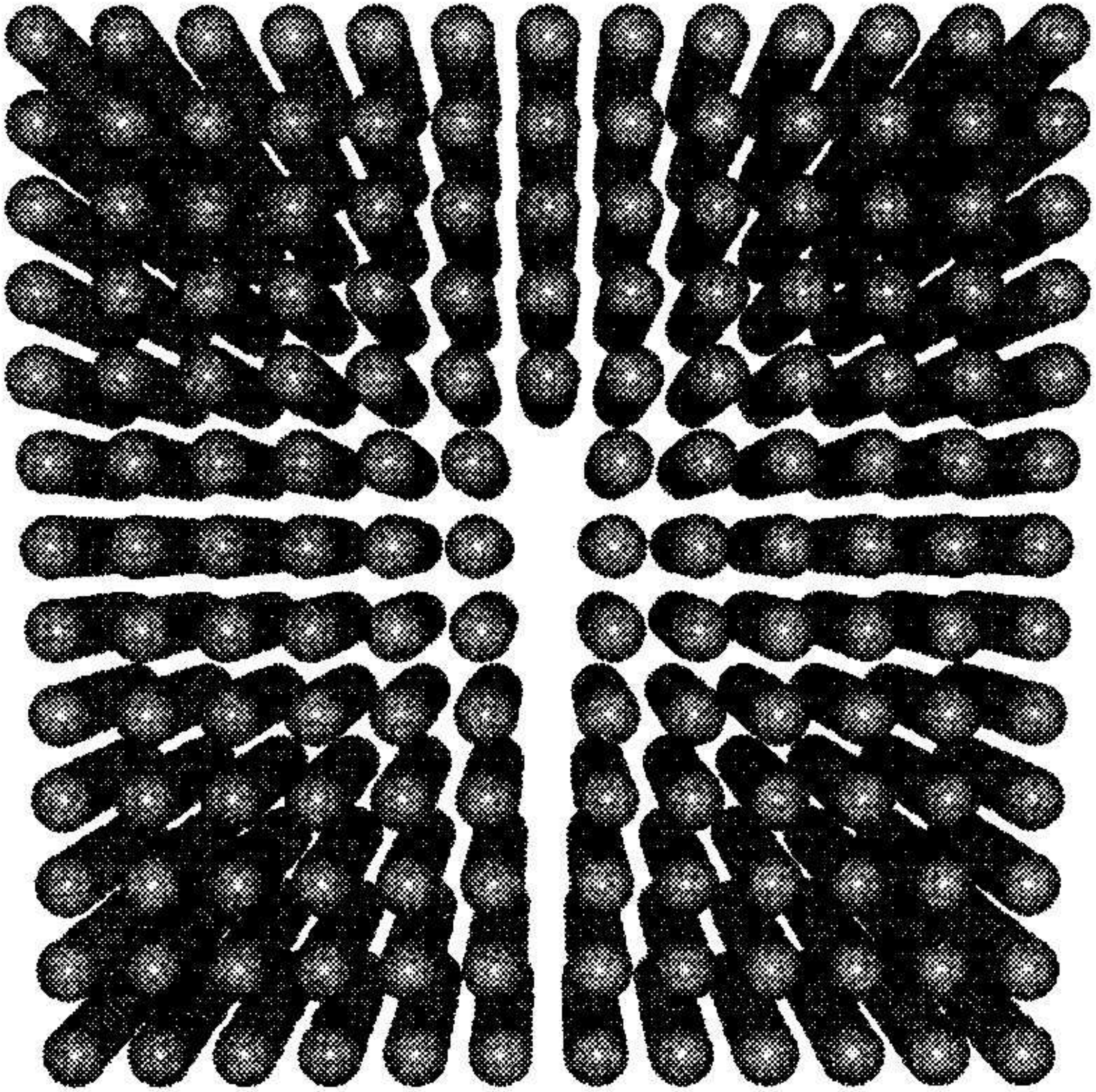

Fig. A.6 Schematic representation of an edge dislocation.

Motion of edge dislocation through a lattice

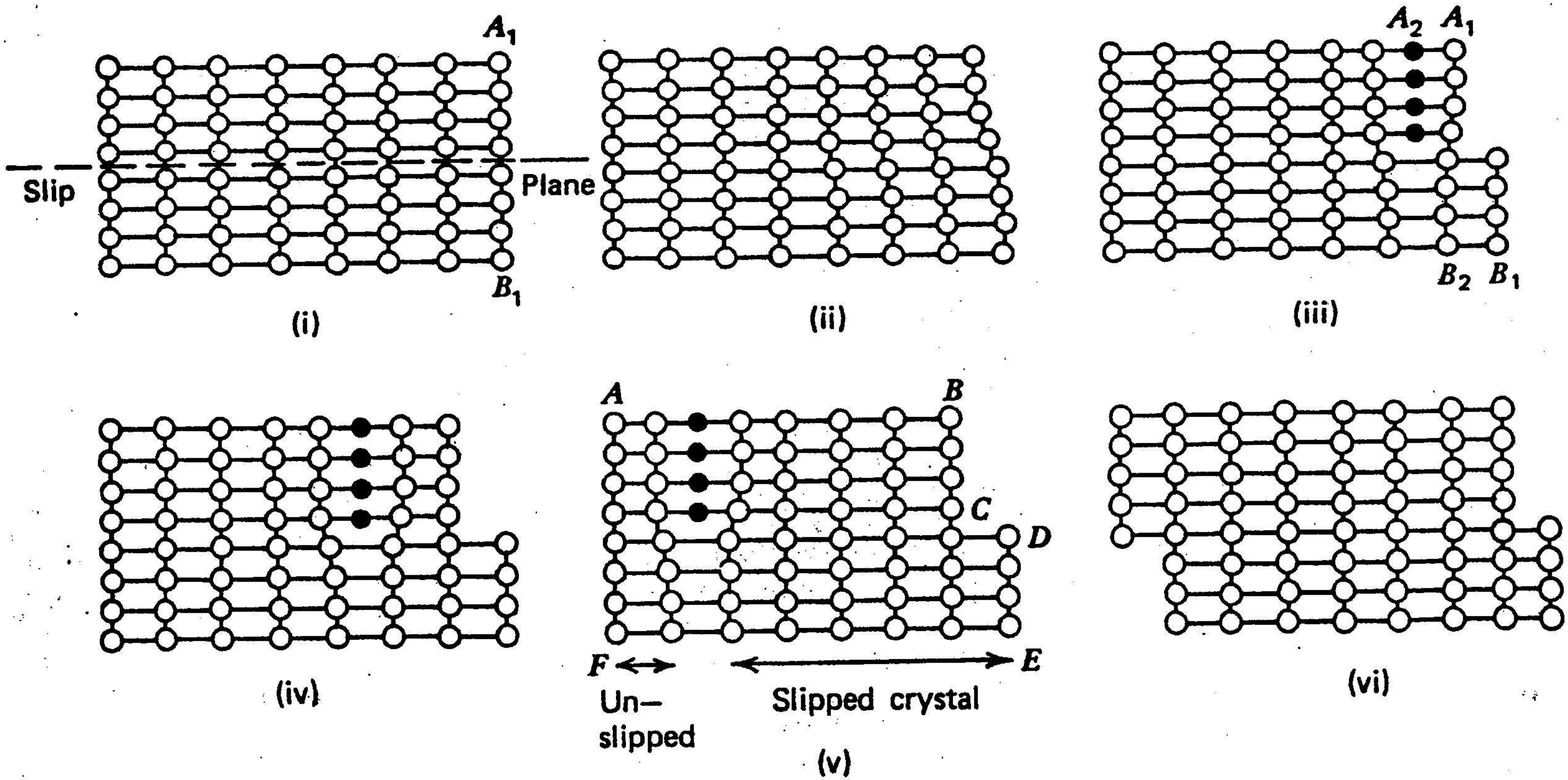

(i) (ii) (iii) (iv) (v) (vi)

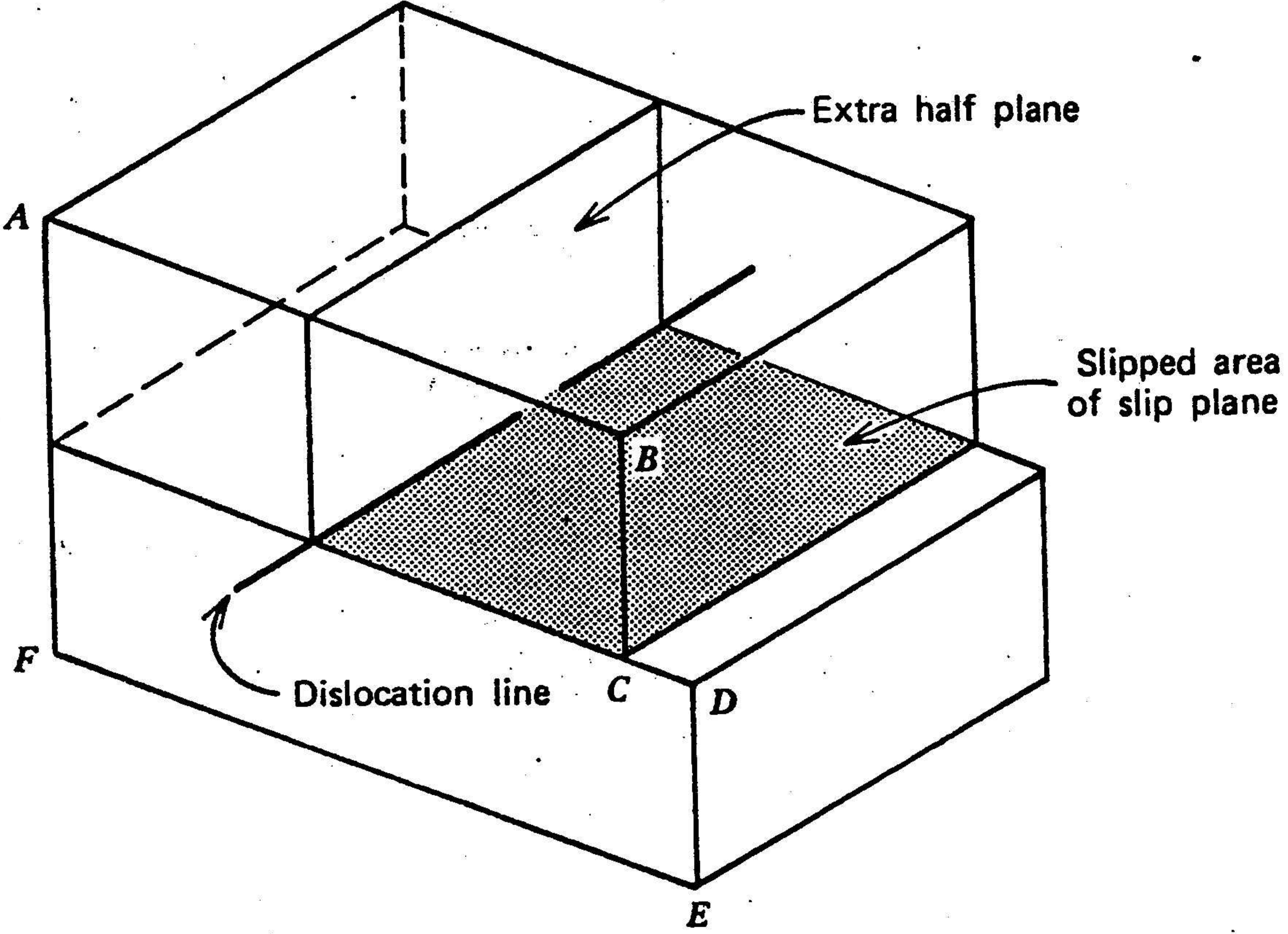
Extra half plane
A
Slipped area of slip plane
B
F
Dislocation line
C
D
E

Propagation of a screw dislocation

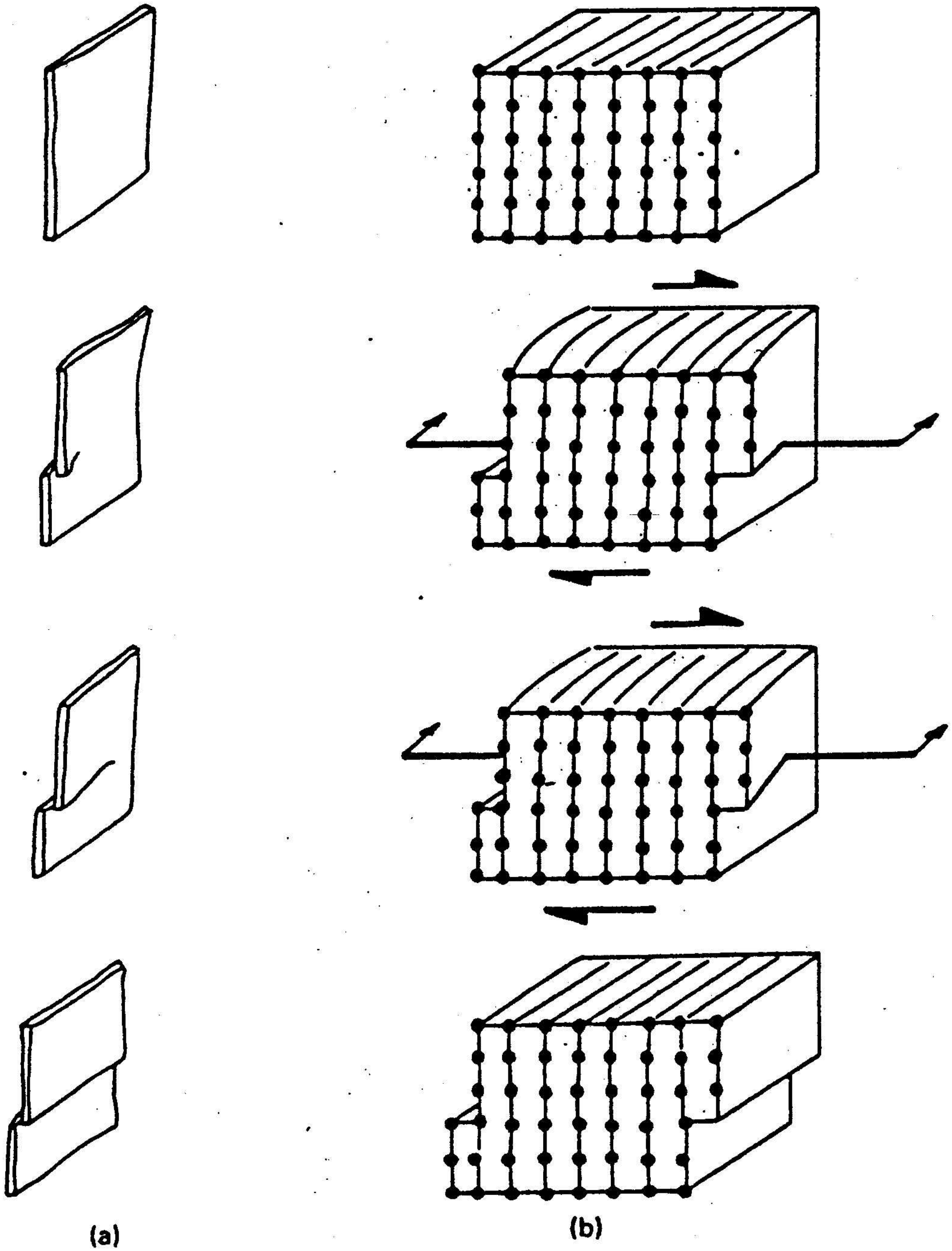

Edge and screw dislocations on the same slipped patch

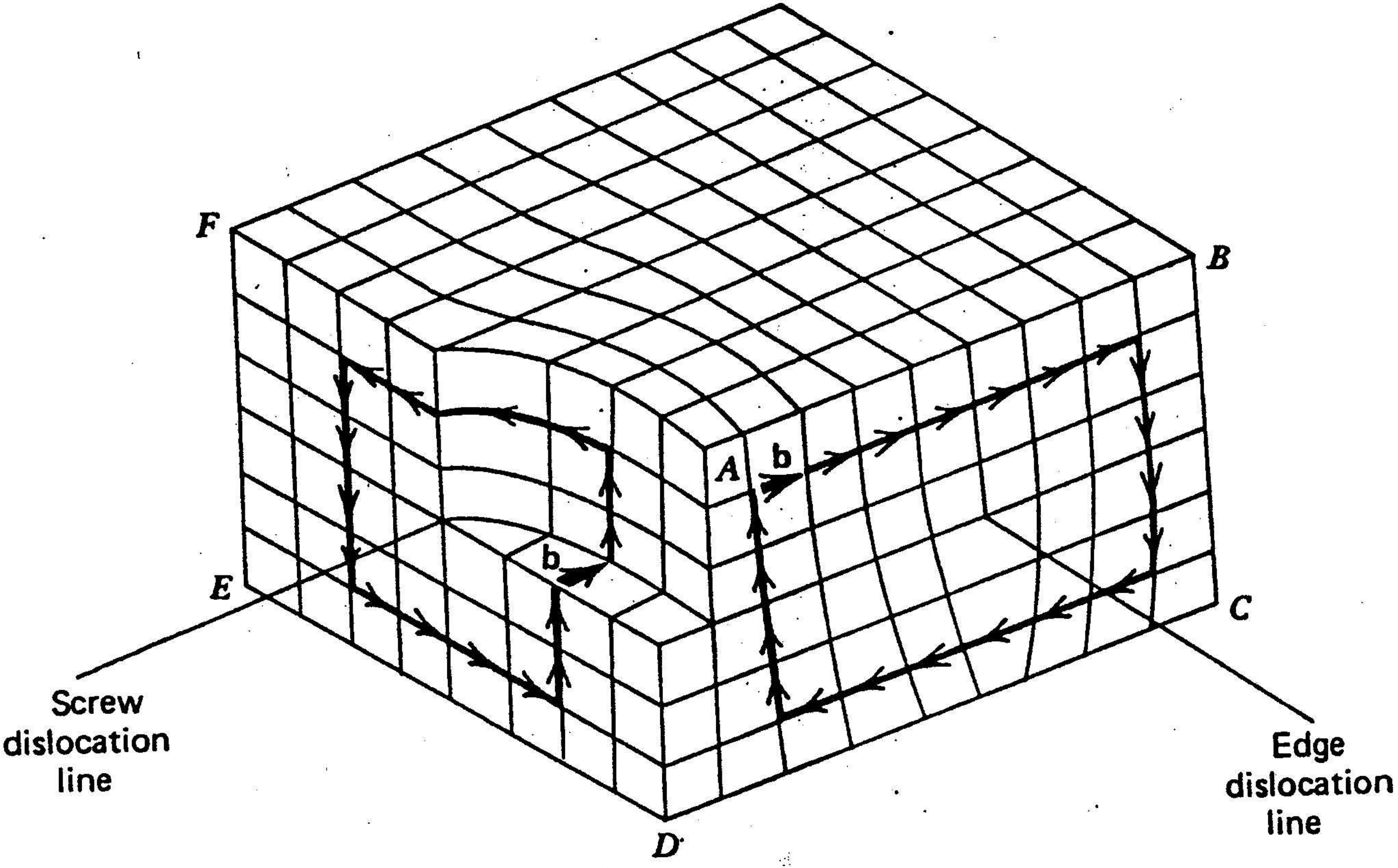

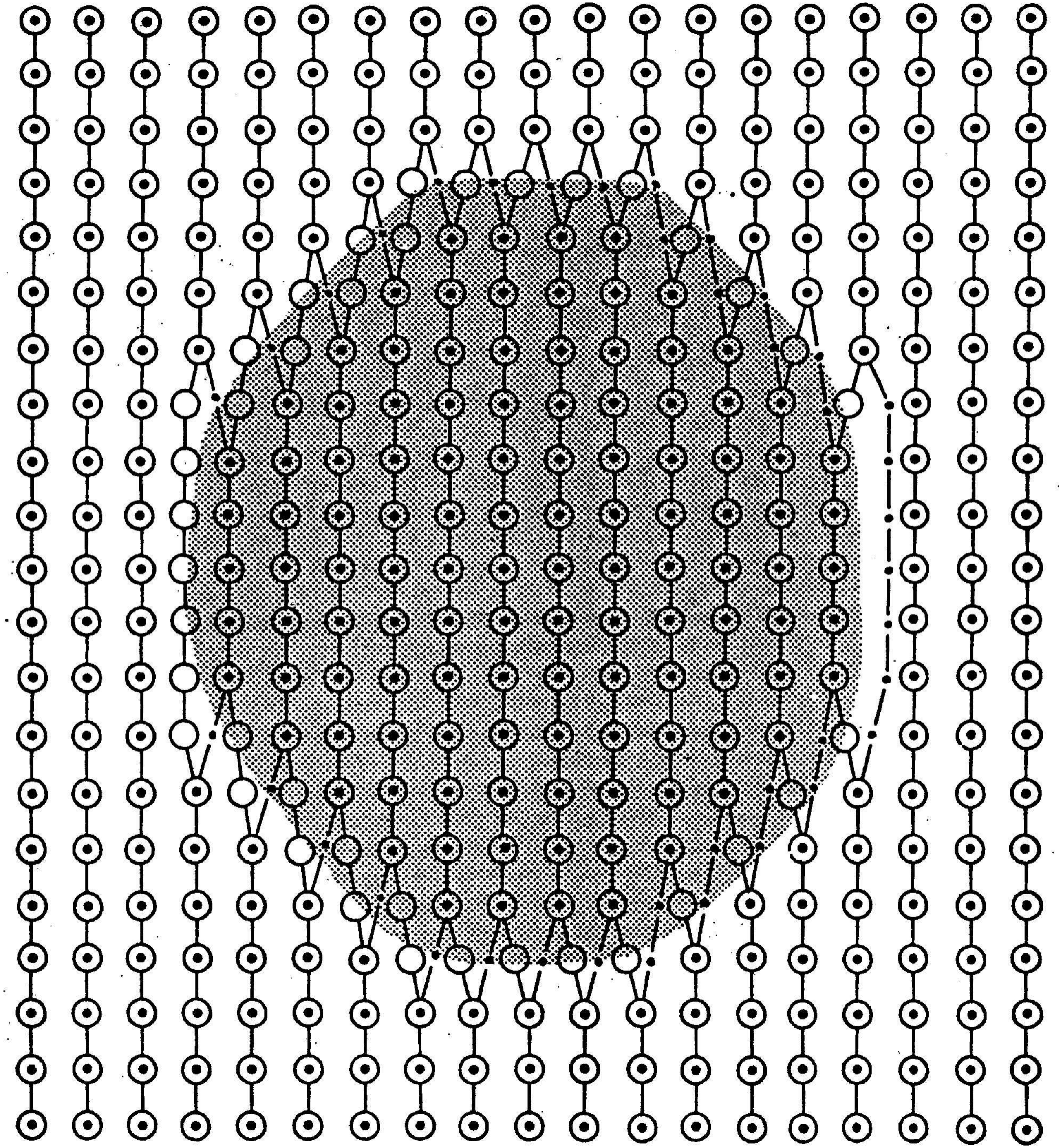

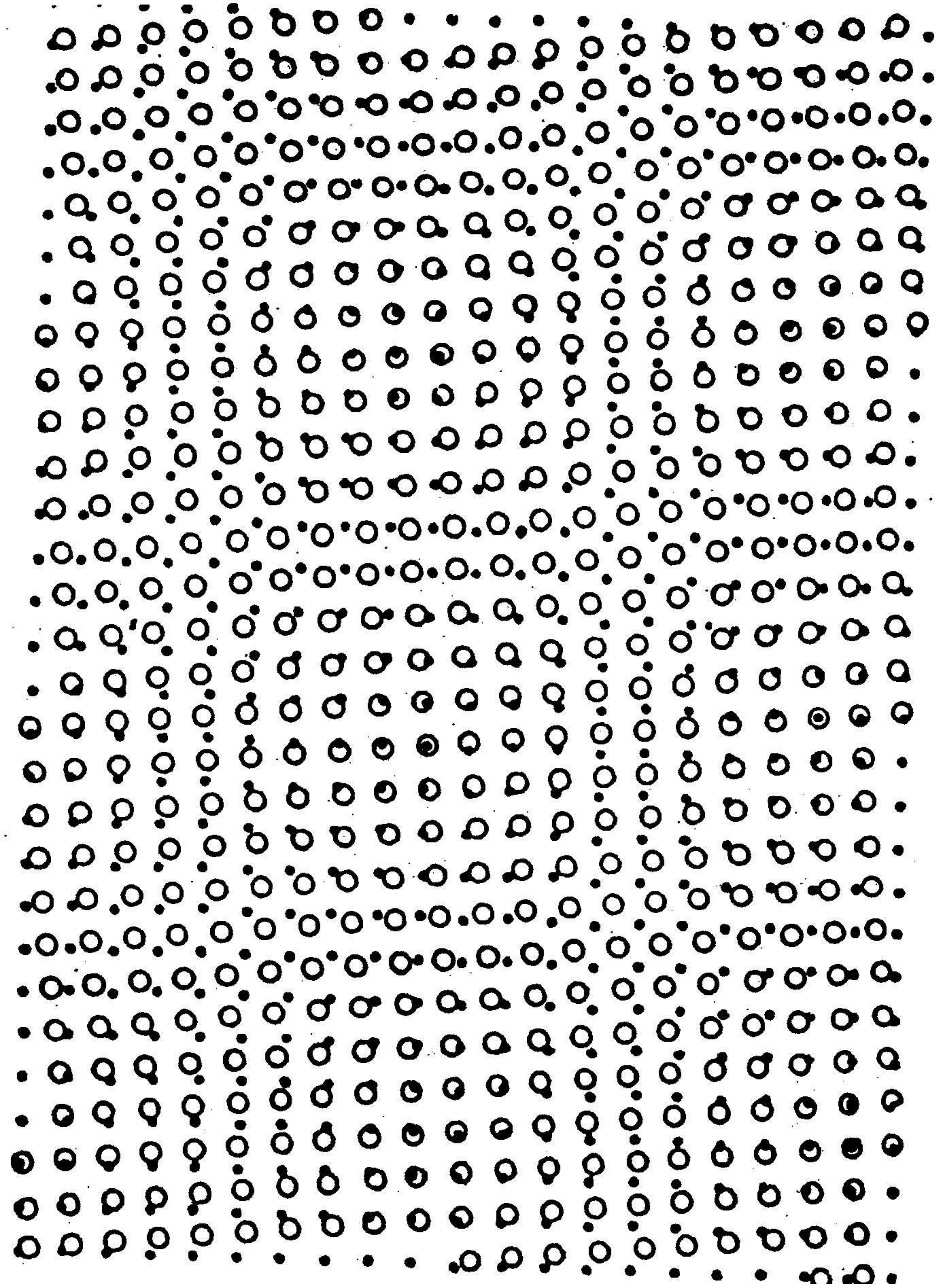

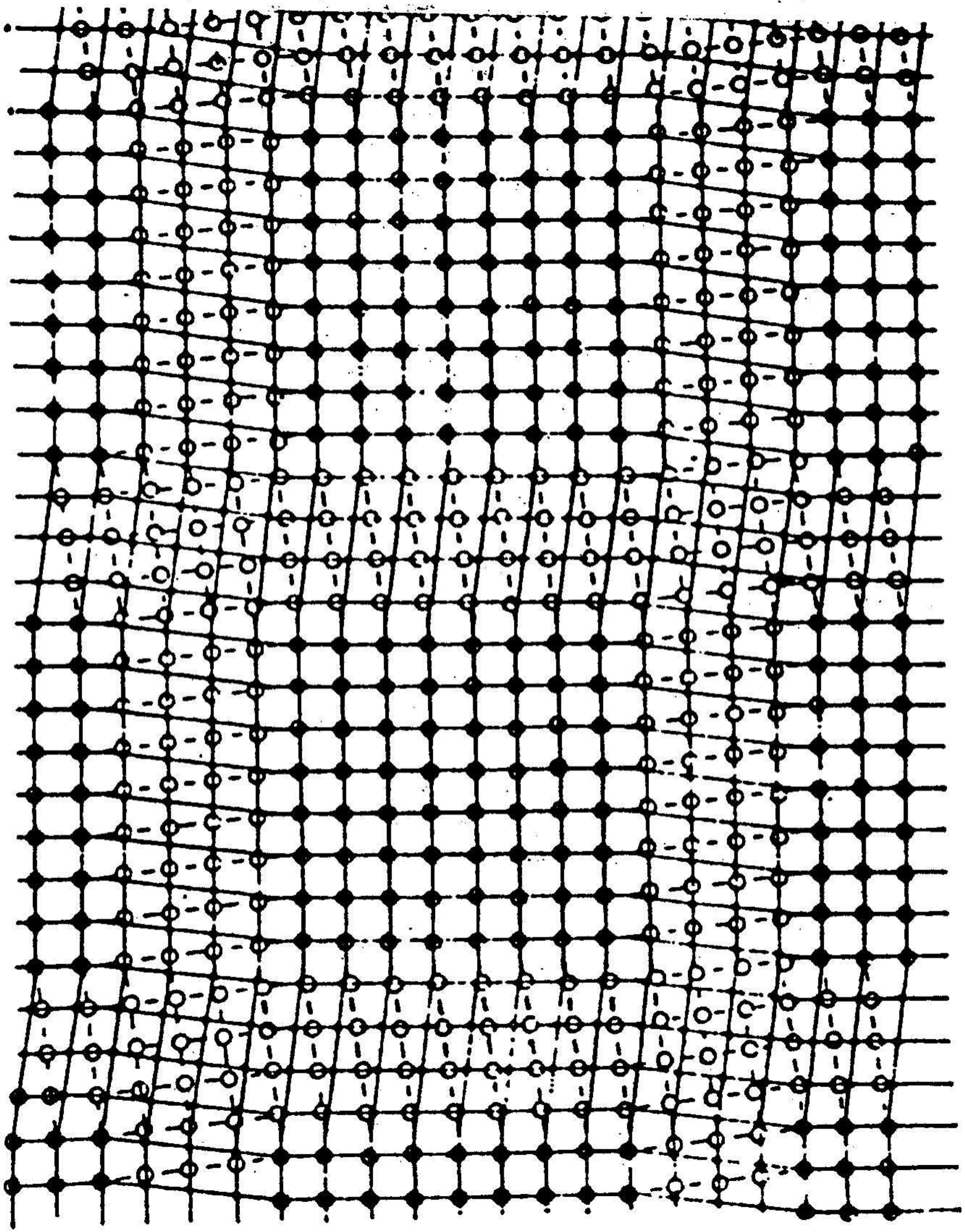

Planar defects

- Grain boundaries
- Twin planes
- Subgrain boundaries
- Deformation bands/lamellae
- Bohm lamellae
- Stacking faults

Unstrained lattice

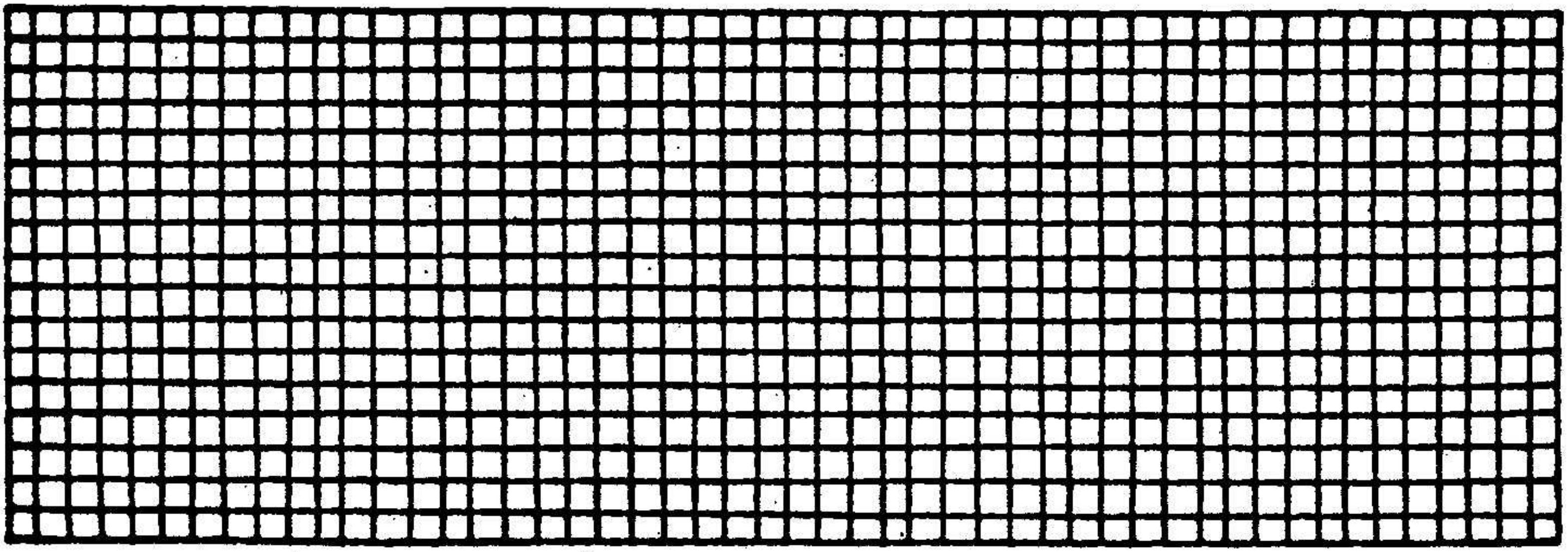

(a)

Elastically strained lattice

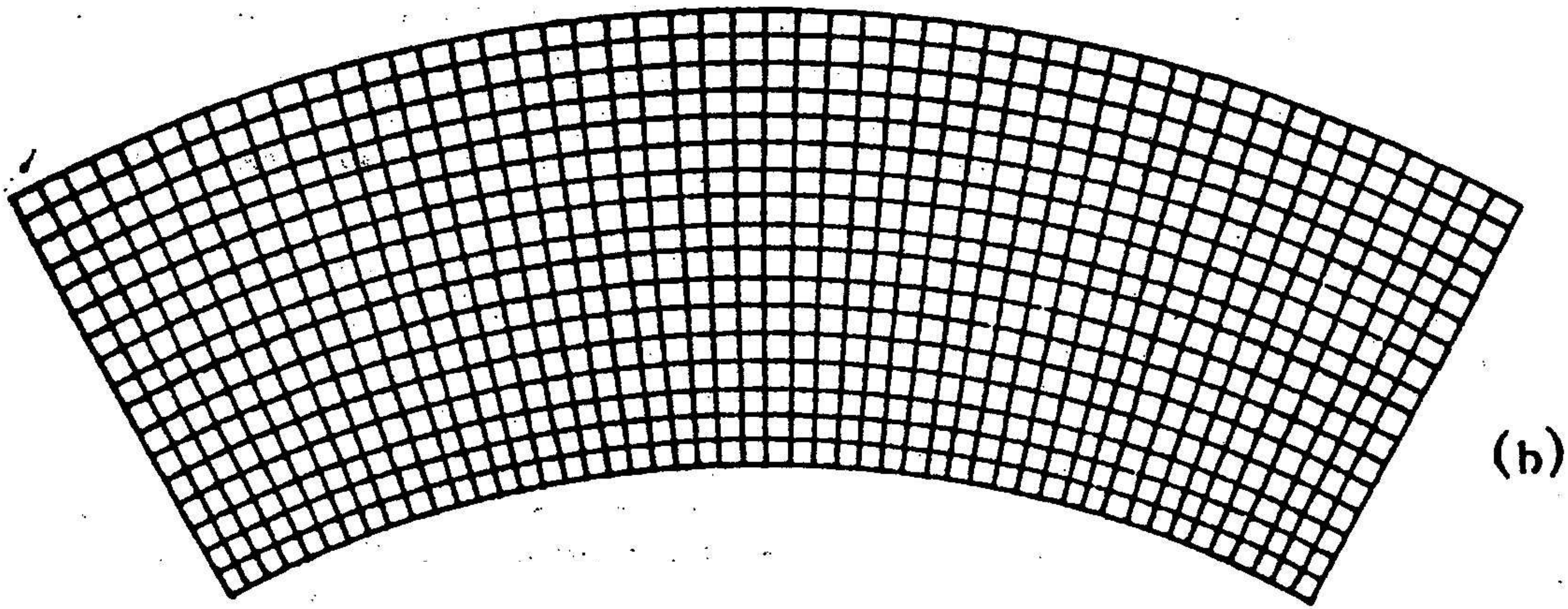

Plastically strained lattice

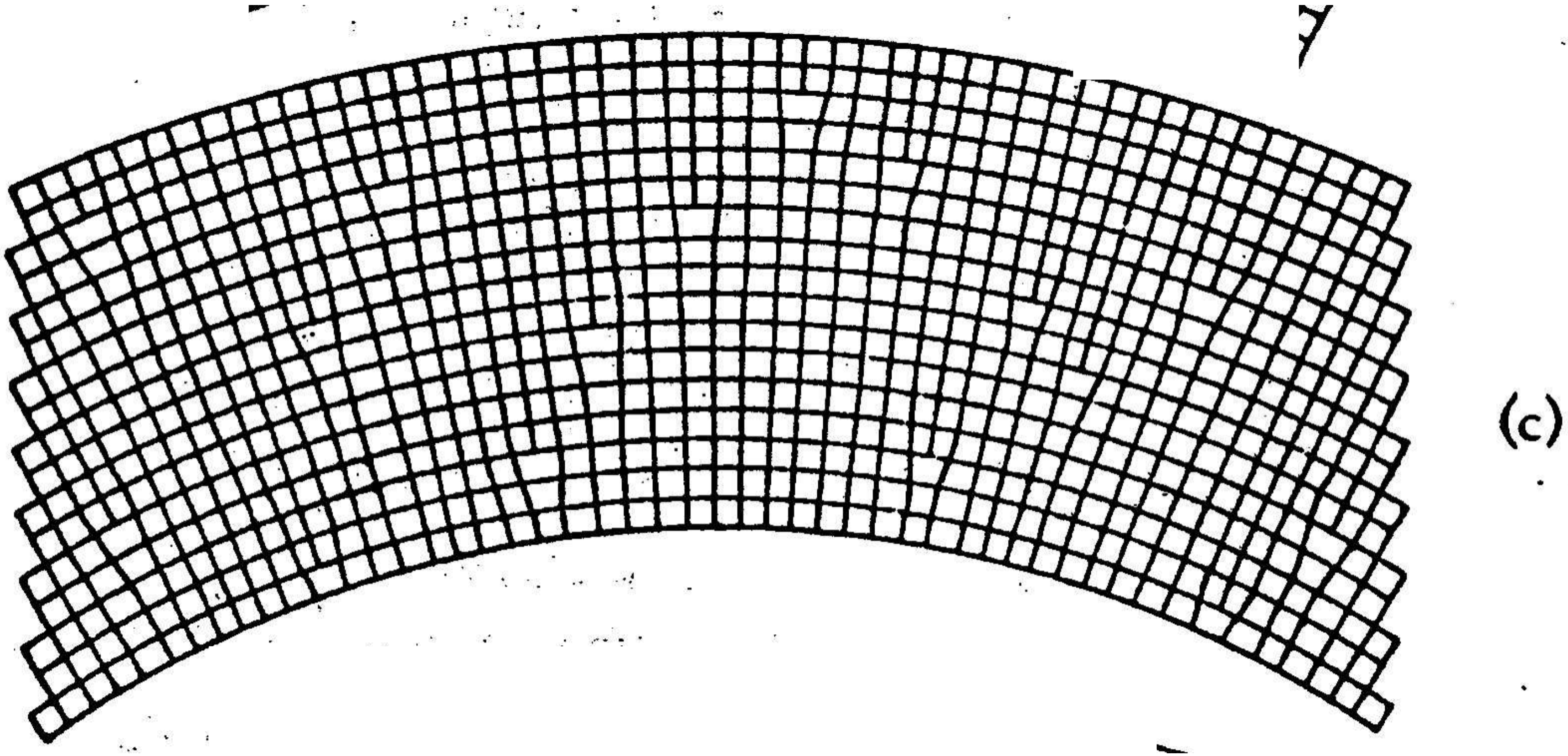

Poligonized lattice

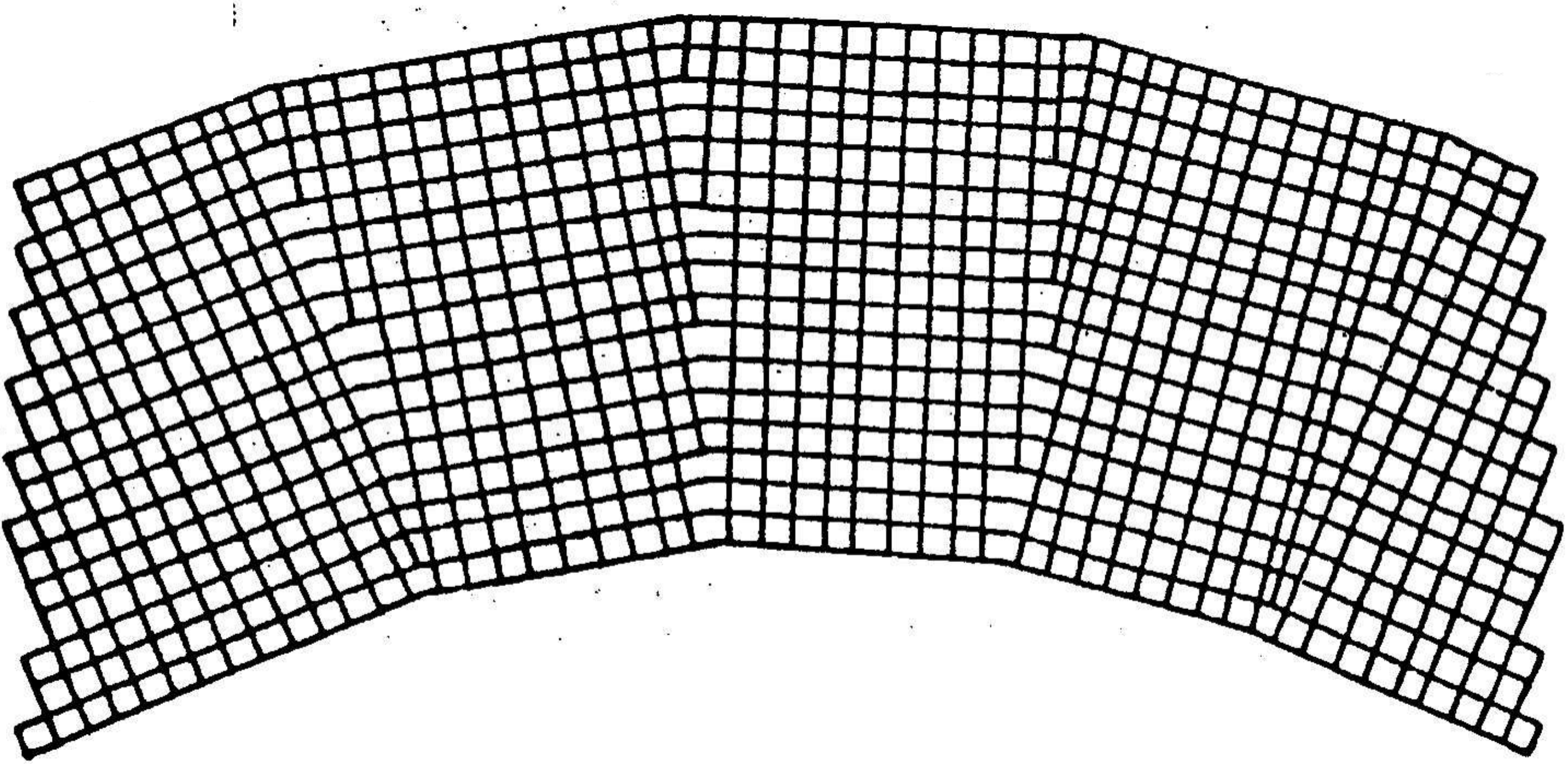

(d)

Edge Dislocations of Opposite Sign Within Same Slip Planes

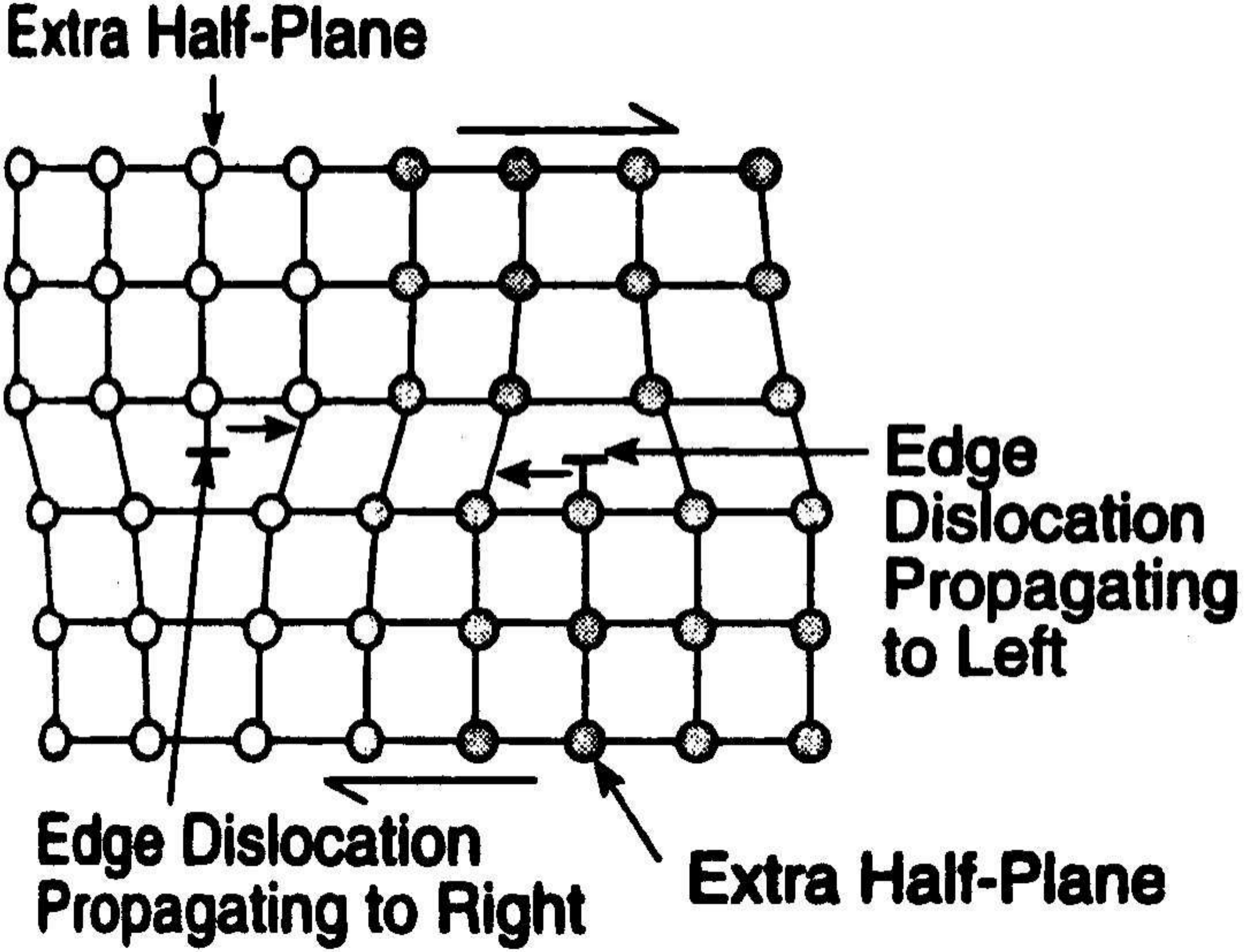

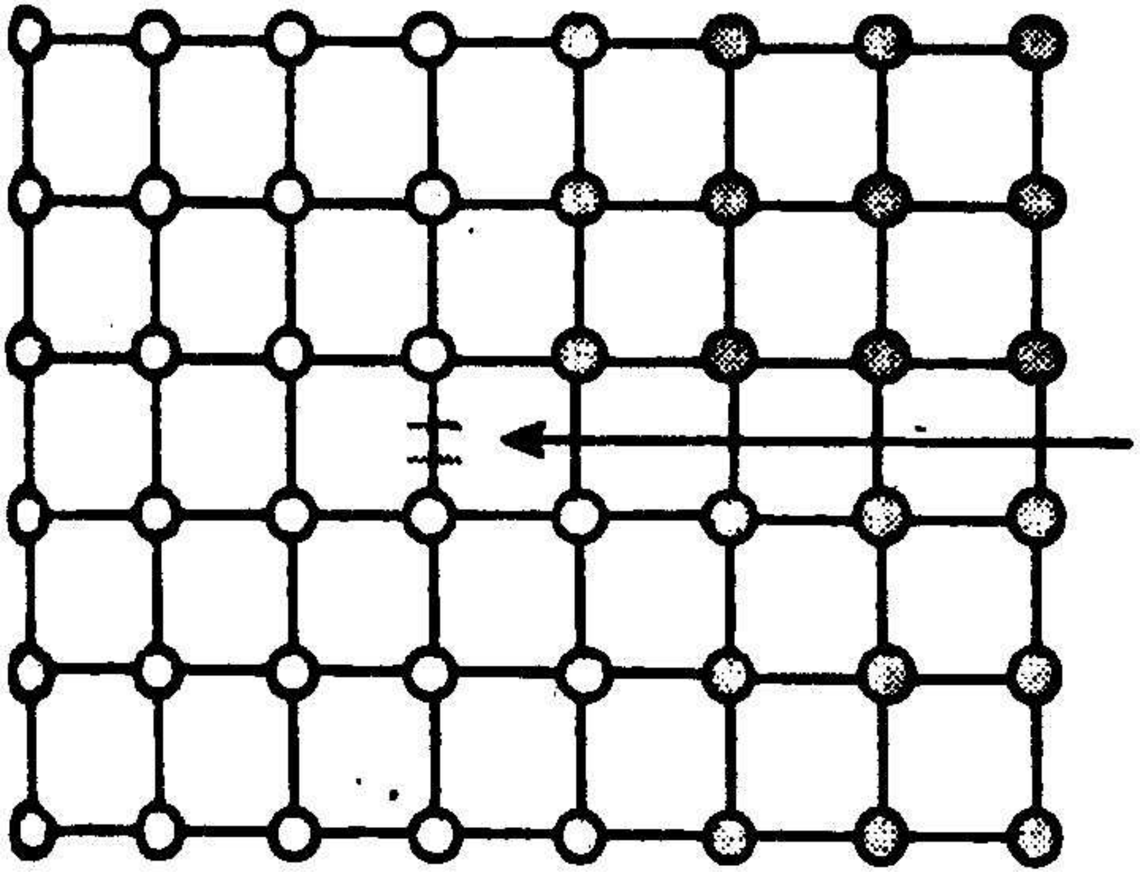

Dislocations Cancel Each Other and Lattice is Healed

Edge Dislocations of Opposite Sign Within Different Slip Planes

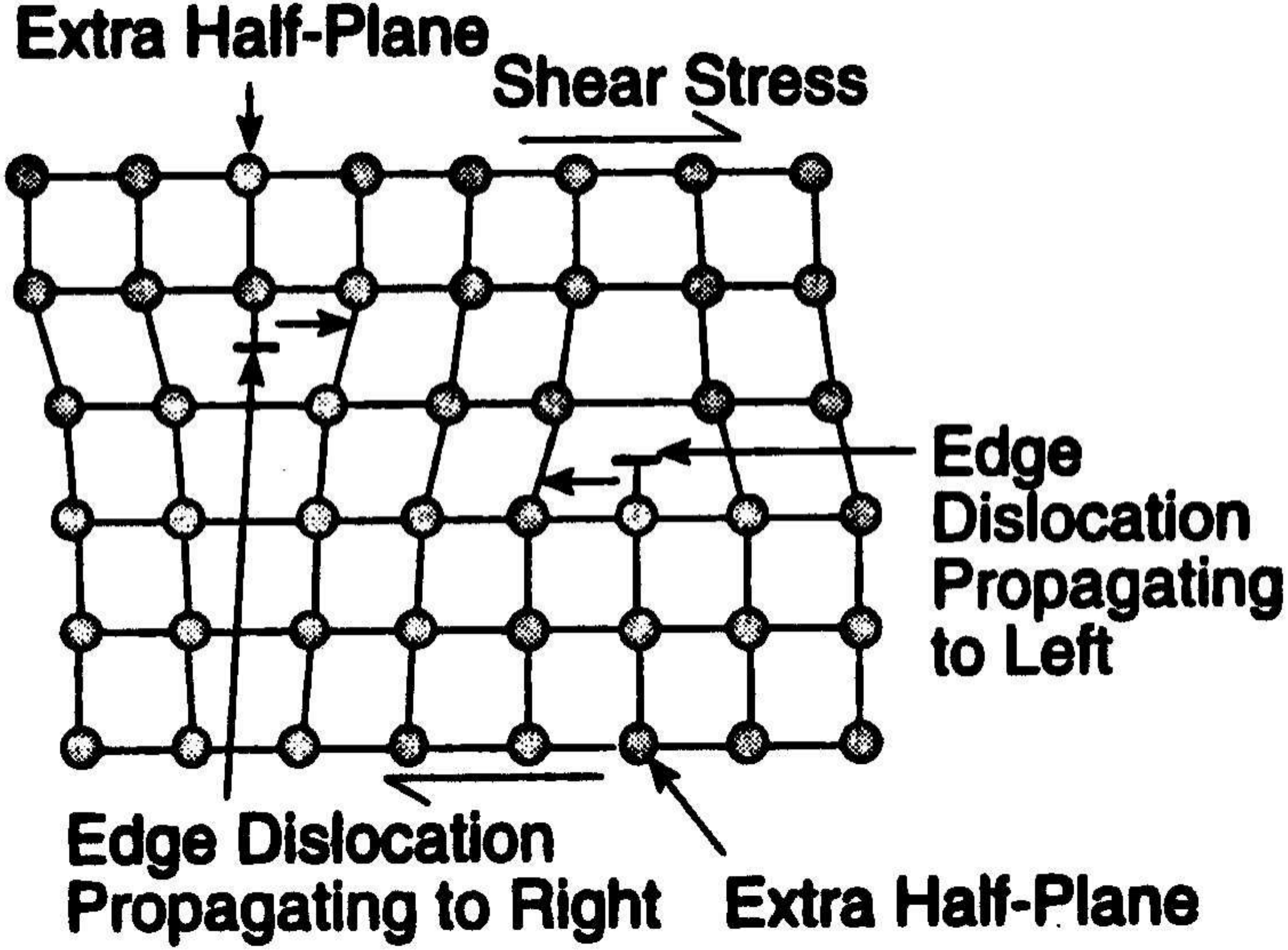

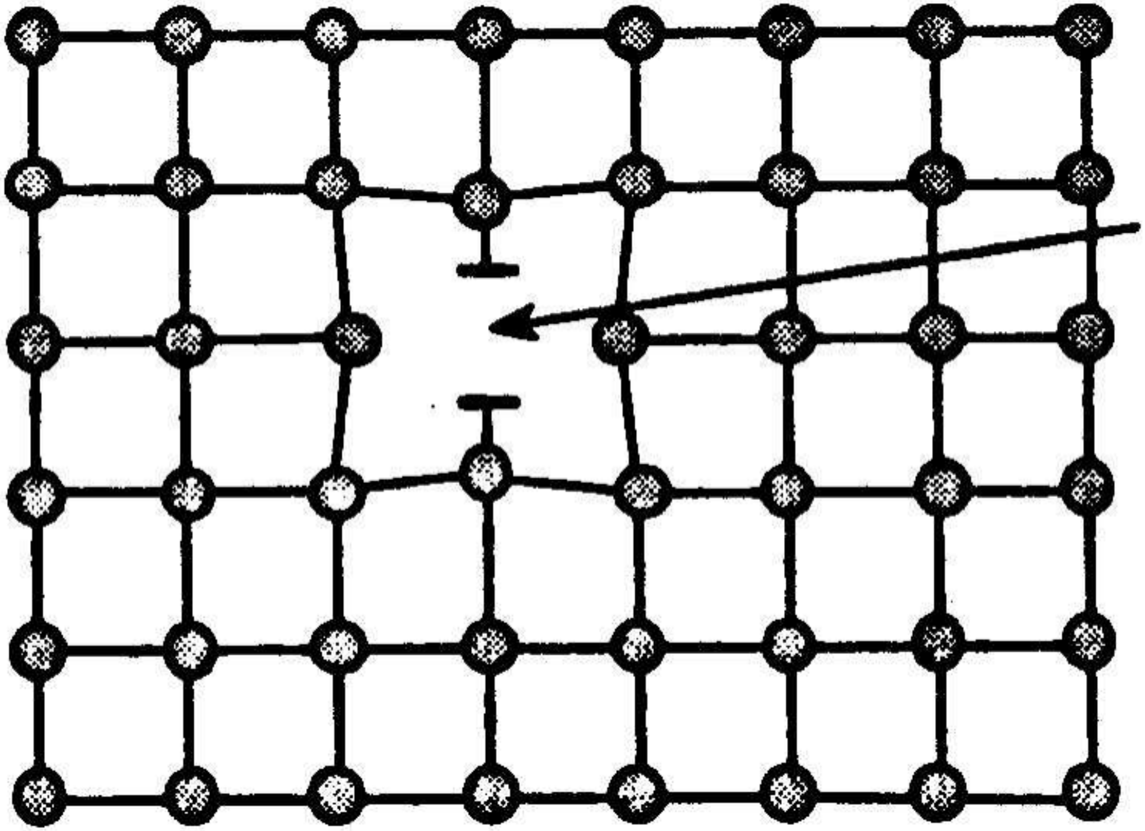

Dislocations Meet and Produce a Line of Vacancies

Edge Dislocations of Opposite Sign with "Overlapping" Half-Planes

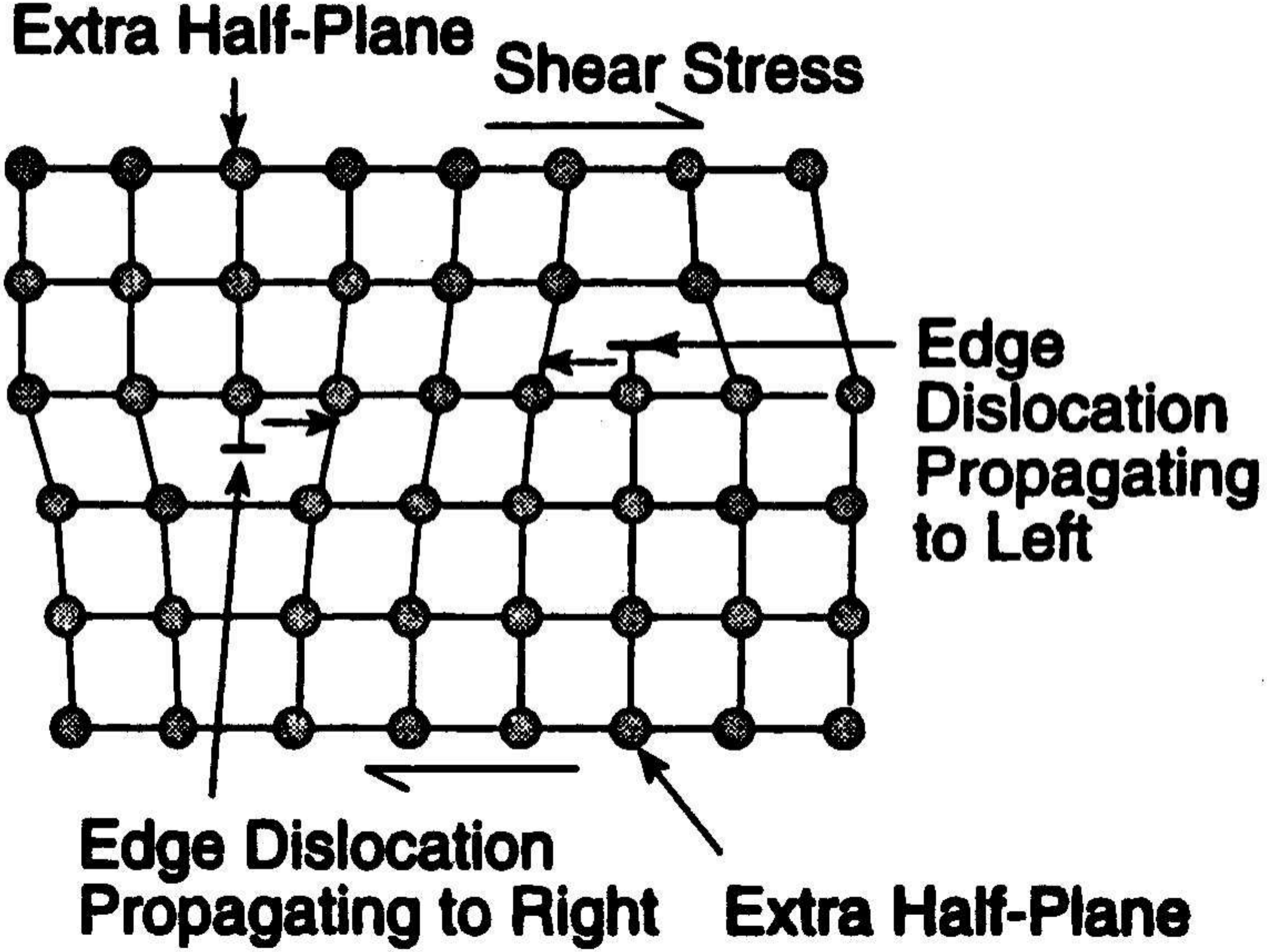

Dislocations Become Locked and Remain in Lattice, Resulting in Strain Hardening

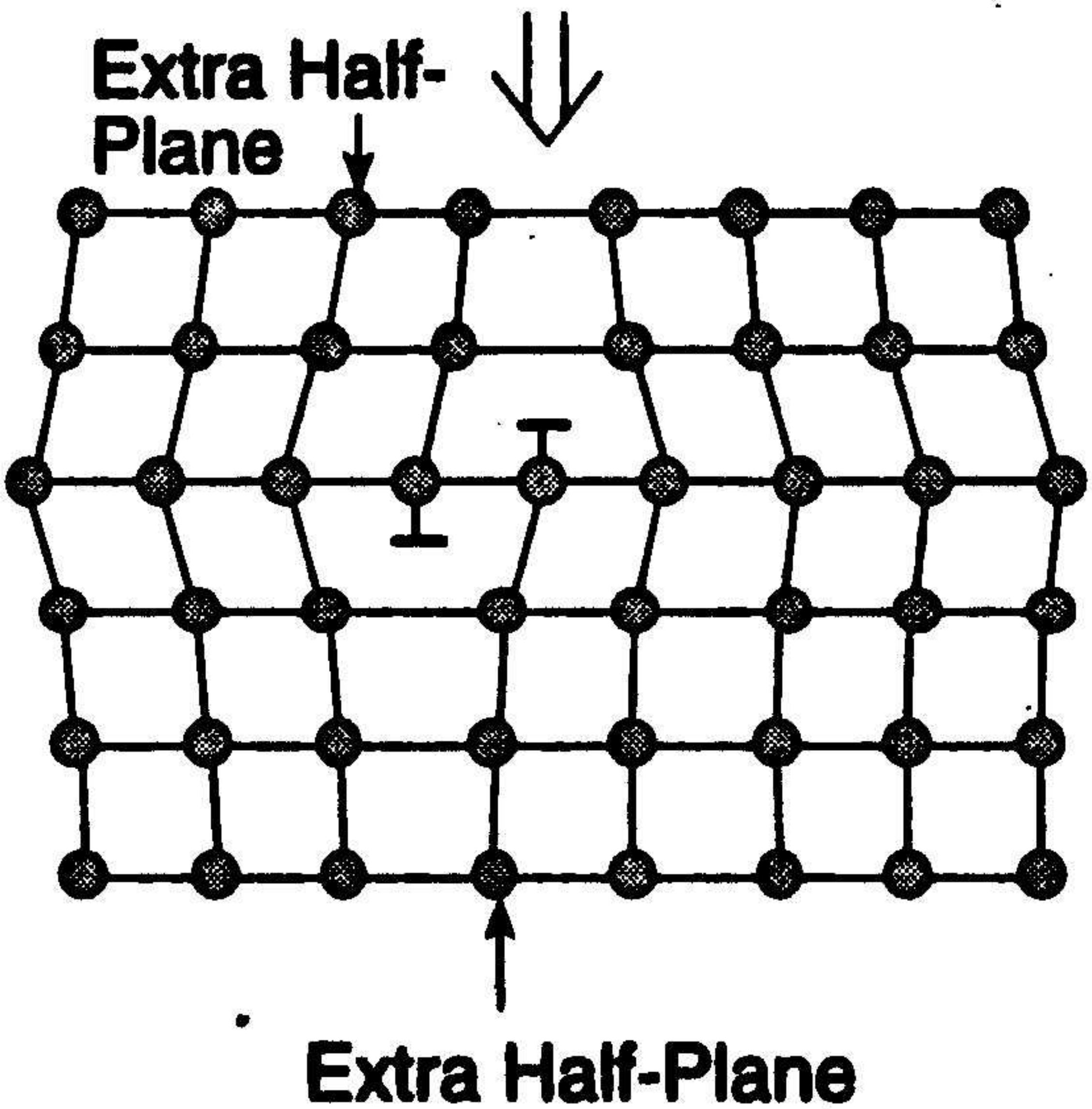

Note: If Either Half-Plane can Shorten via Climb, then the Lattice is Healed

Jog in an edge dislocation

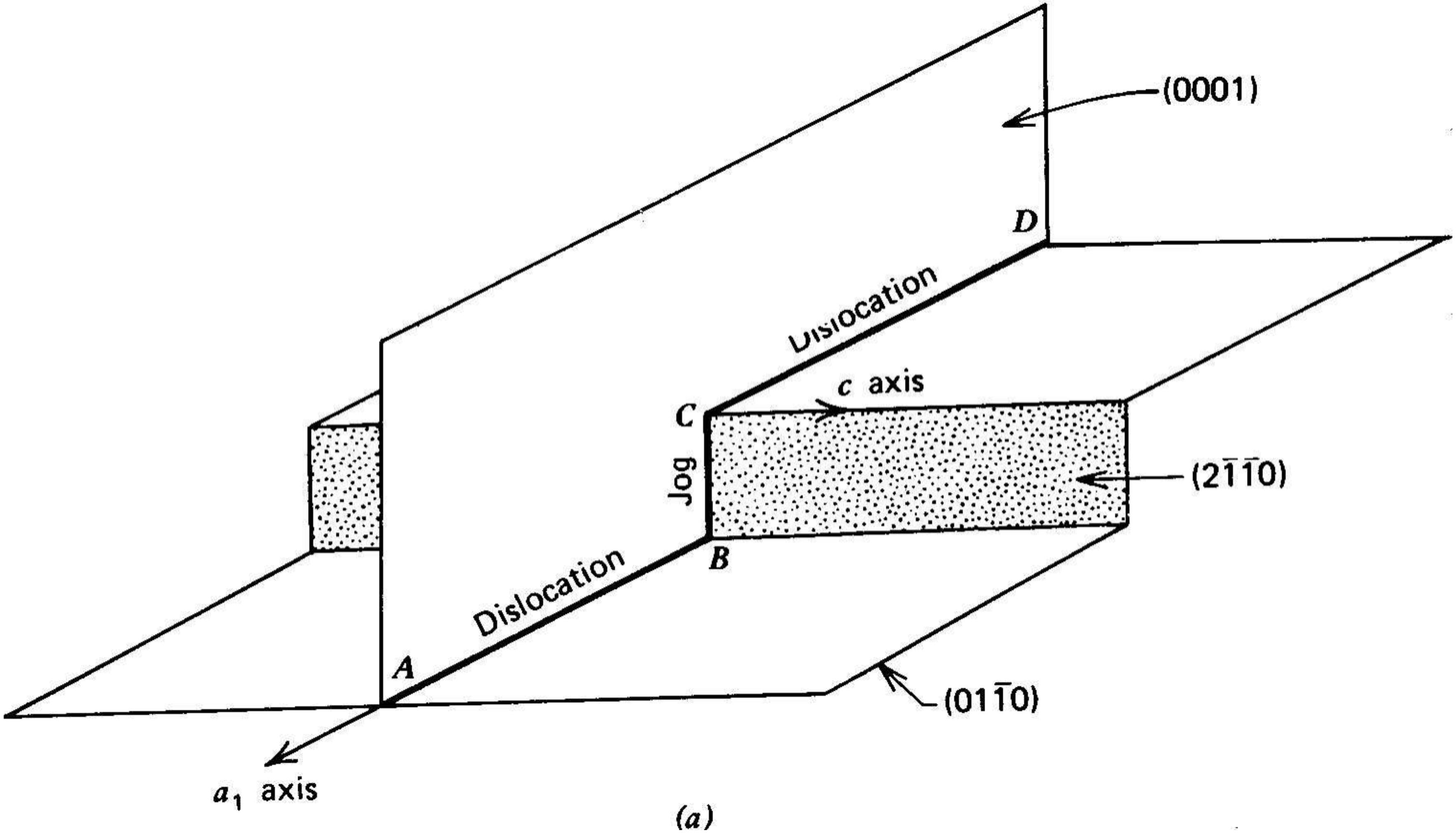

(a)

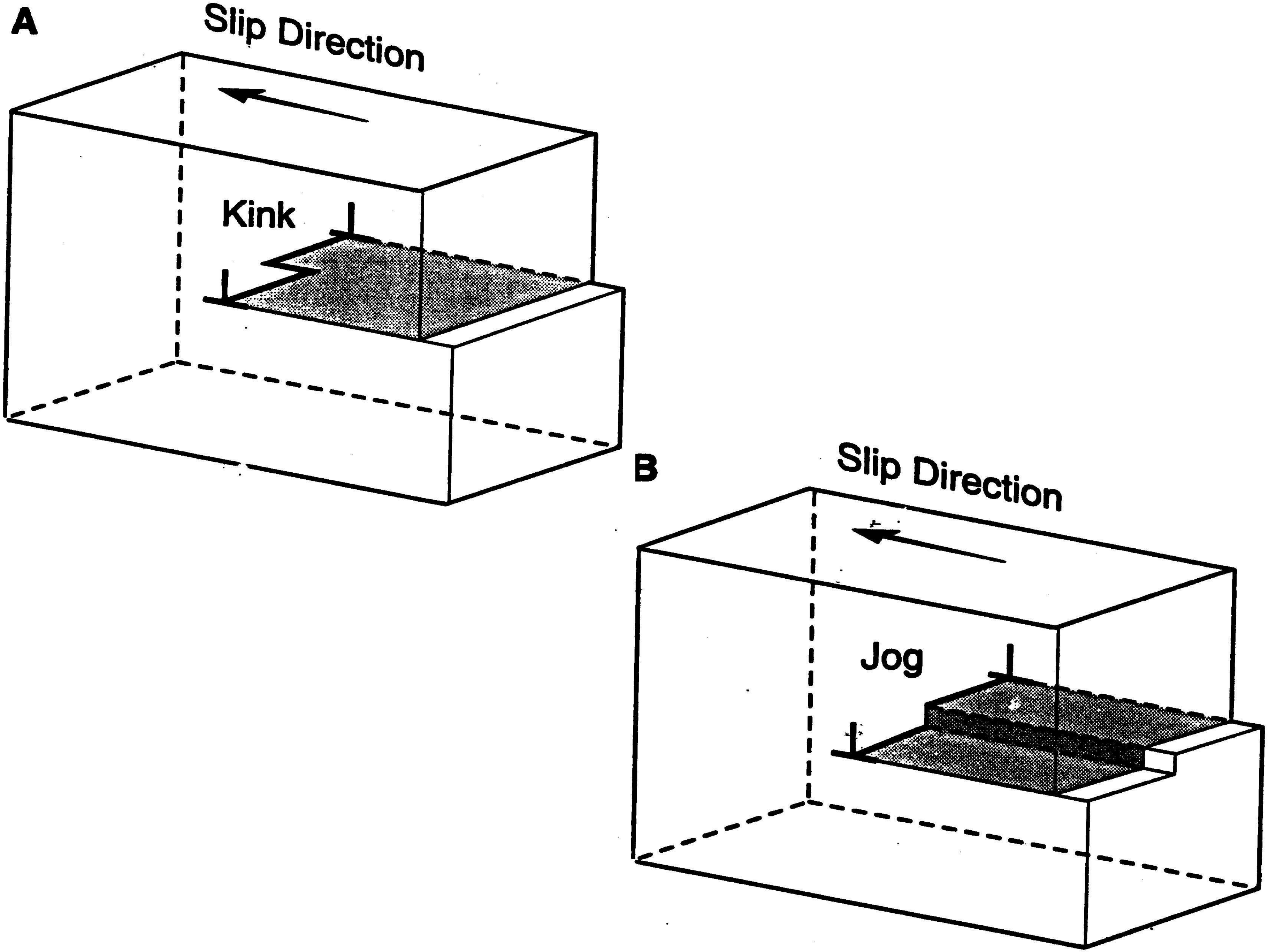
A
Slip Direction
Kink
B
Slip Direction
Jog

Recovery

Processes occurring between 0.3-0.5 Tm that reduce dislocation density (and hence reduce the elastic strain energy inside of a crystal). Work hardening (tangling of dislocations) competes with recovery.

- ***Vacancy diffusion*** helps untangle dislocations
- ***Climb*** to straighten and untangle dislocations
- Dislocation anihilation
- Ordering of dislocations into walls
- Subgrain formation

Unstrained, recovered lattice

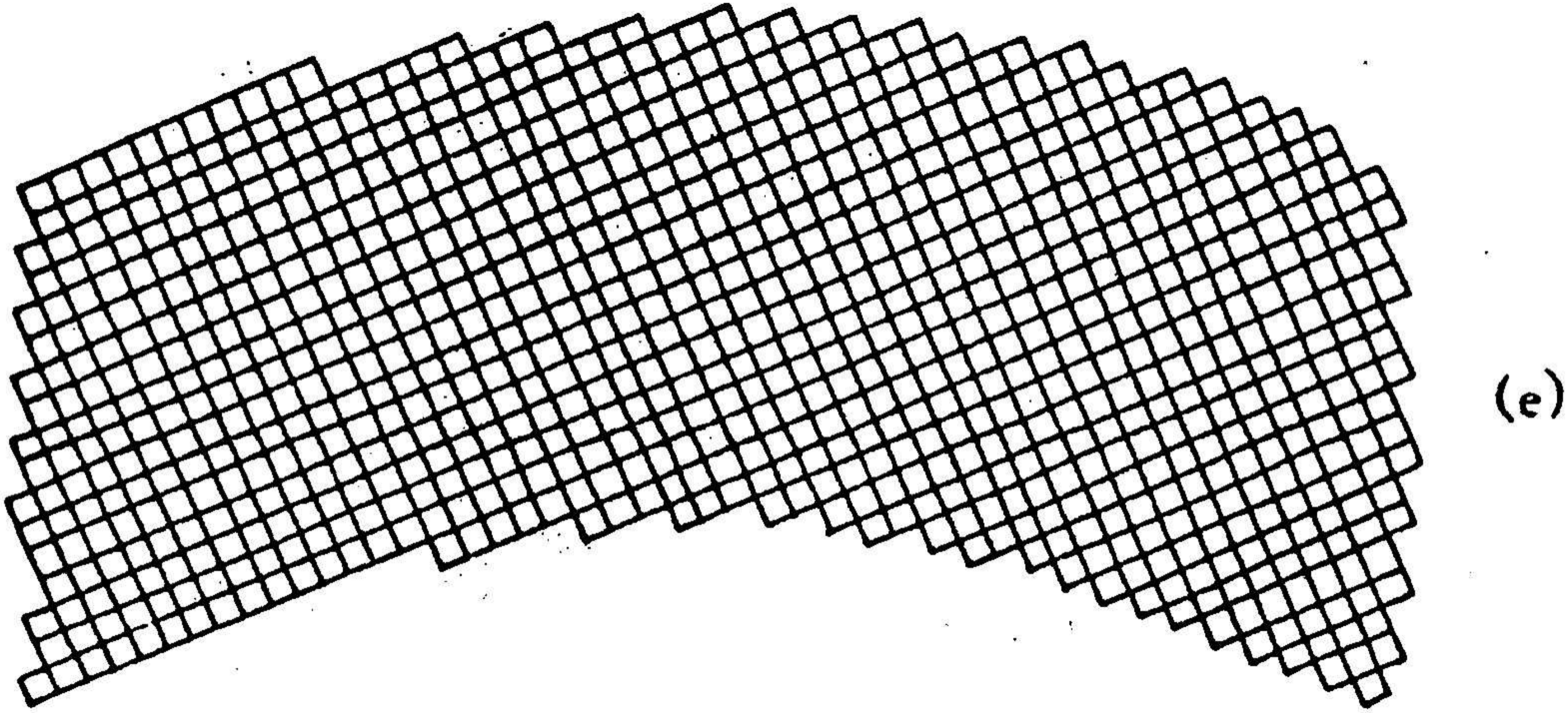

Dislocation creep = dislocation glide + dislocation climb

The motion of dislocations and vacancies through a crystal occurs at all temperatures, but it is much faster at high temperatures than at low temperatures.

Dislocation creep = dislocation glide + dislocation climb

At high temperatures, it takes less energy for vacancies to diffuse through or around a crystal.

The amount of strain energy needed to break chemical bonds

Competing Processes

Work Hardening:

dislocations tangle and obstruct each others' motion. Strain leads to an increase in dislocations, inhibiting further strain.

Competing Processes

Work Softening:

dislocations are anihilated or organized into subgrain boundaries (tilt walls), resulting in lattices that contain fewer dislocations.

Recovery and **recrystallization** are involved; enhanced at higher temperatures.

Homologous Temperature (Tm)

This is the melting temperature of a mineral expressed in the Kelvin temperature scale:

0 K = -273.16°C

Zero Kelvin is called ***absolute zero***, because it is the temperature at which the volume of any ideal gas would reach zero and at which all thermal vibration of

Primary Recrystallization

Occurs at temperatures above half the homologous temperature (Tm) for a mineral.

- Grain boundary area reduction (GBAR)
  - Grain boundaries are straightened and flattened
  - Ratio of volume to surface area is maximized for given physical and chemical conditions
- Equilibrium is approached, given enough time at high temperature

Dynamic Recrystallization

Processes that reduce the internal strain energy of a crystal and reduce the surface energy along grain boundaries.

- Grain boundary migration recrystallization (GBM)
- Subgrain rotation recrystallization (SR)

Dynamic Recrystallization

...under *high* flow stress results in ***smaller*** crystals

Dynamically recrystalized rocks with smaller crystals are typically stronger and denser than they were before deformation.

MOUNT BURNET DUNITE ("dry")

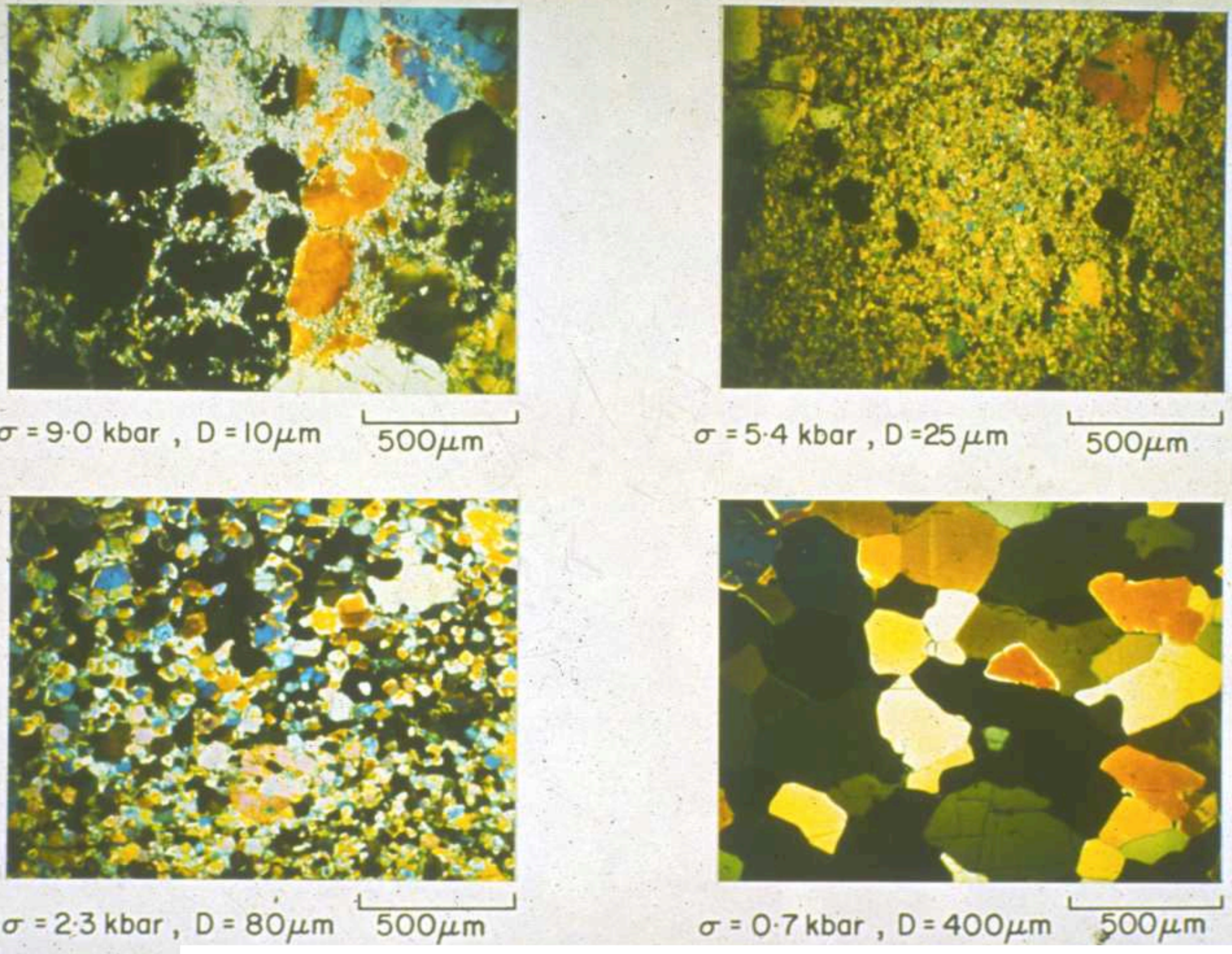

$\sigma = 9\cdot0$ kbar , $D = 10\,\mu m$

$\sigma = 5\cdot4$ kbar , $D = 25\,\mu m$

$\sigma = 2\cdot3$ kbar , $D = 80\,\mu m$

$\sigma = 0\cdot7$ kbar , $D = 400\,\mu m$

Texas A&M University Center for Tectonophysics

Flow Laws

Dislocation (or power-law) **creep** modeled with a form of the Dorn equation

$$\dot{\varepsilon} = A\sigma^{n}\, e^{(-Q/RT)}$$

Diffusion creep

- Coble creep (grain-boundary diffusion)
- Nabarro-Herring creep (volume/ vacancy diffusion)

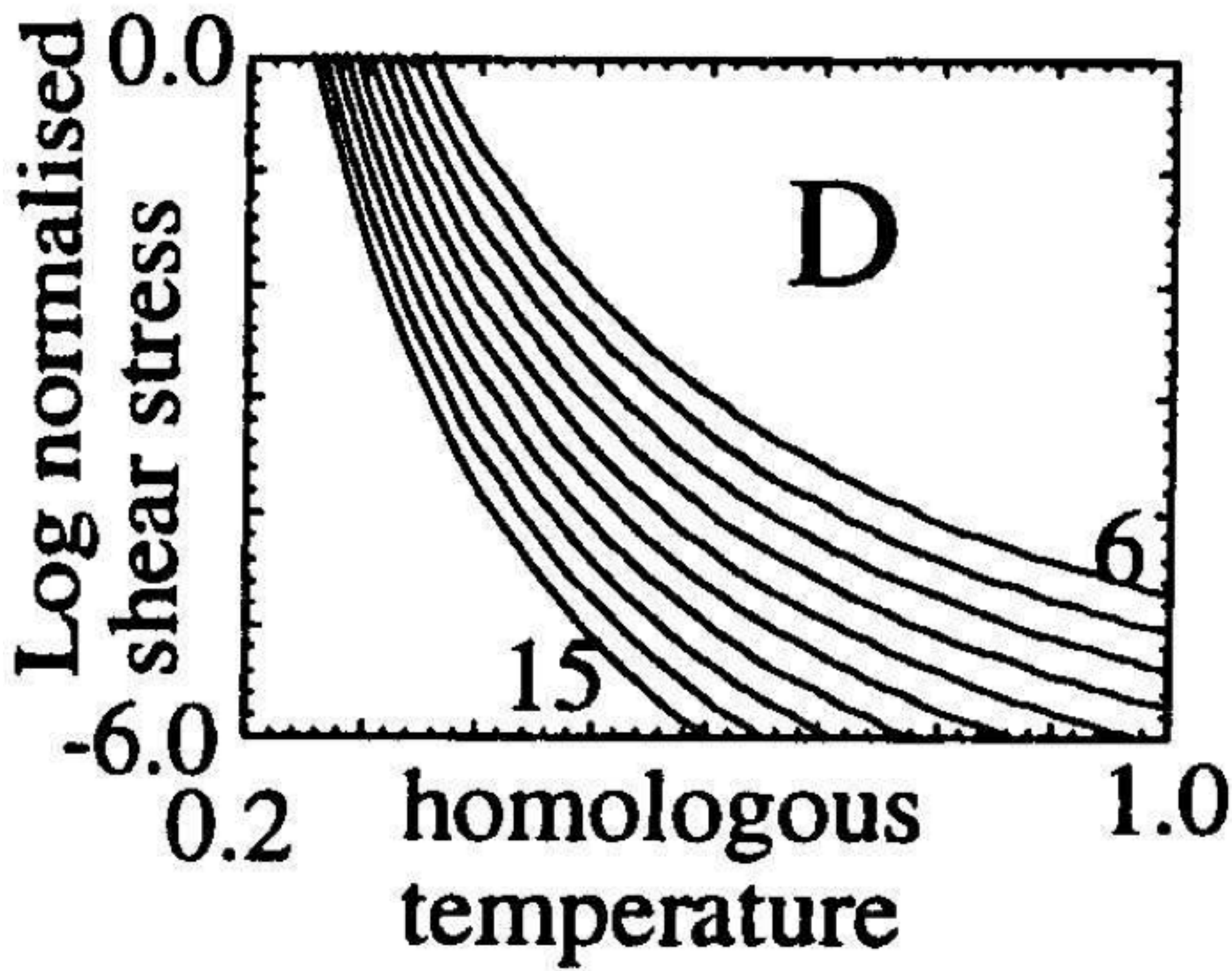
Log normalised shear stress
0.0
-6.0
D
6
15
0.2
1.0
homologous temperature

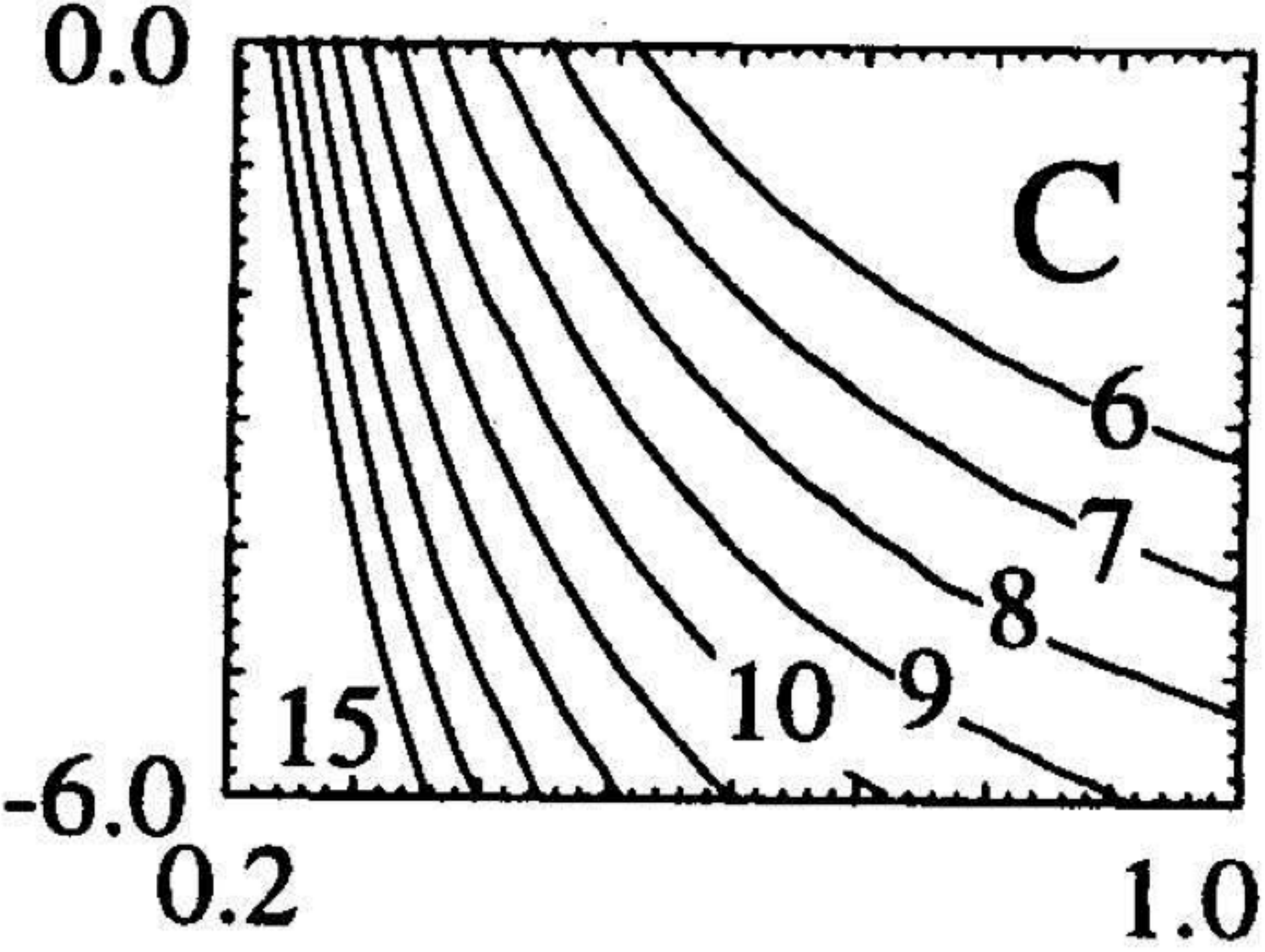
0.0
-6.0
0.2
1.0
C
6
7
8
9
10
15

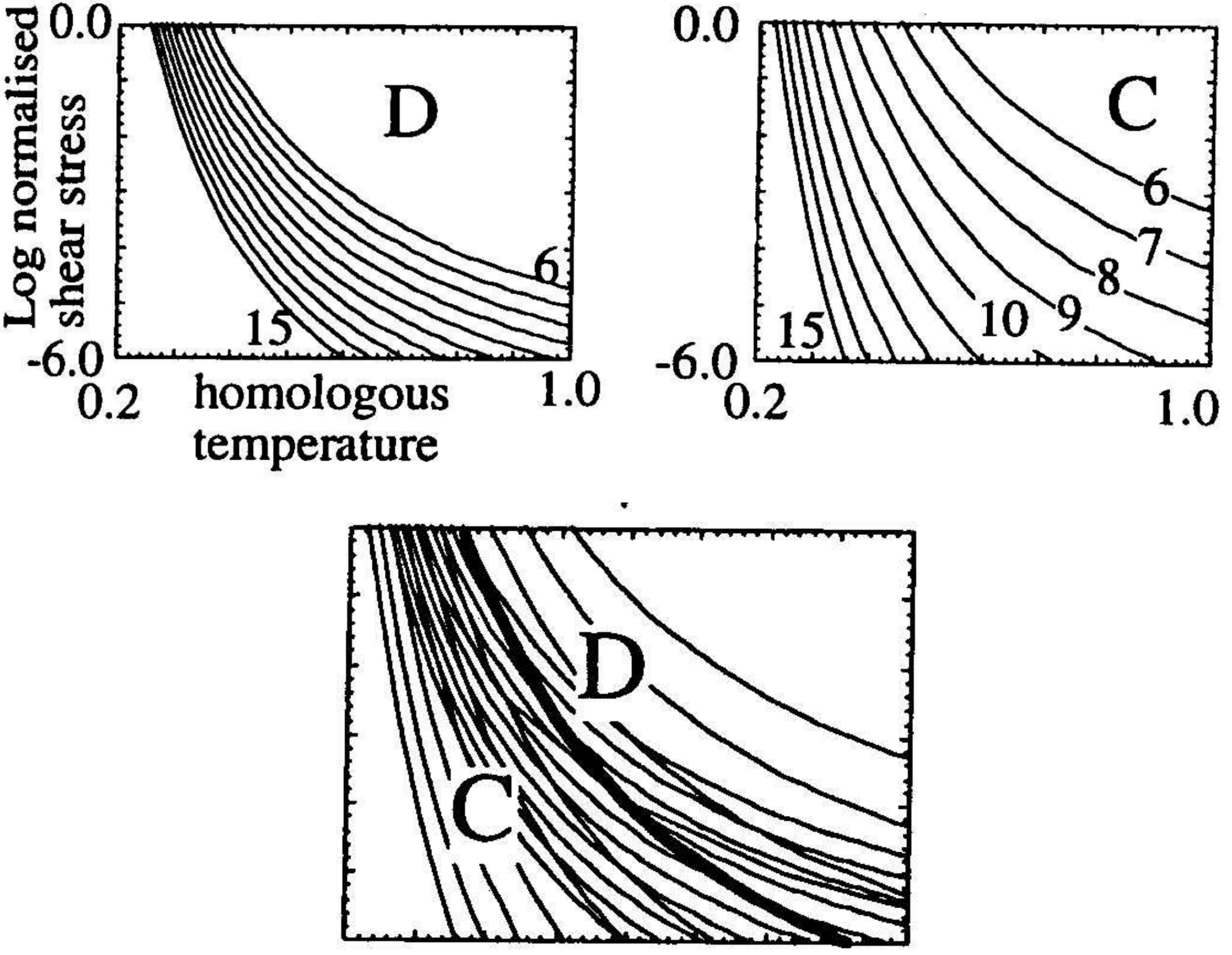
Log normalised shear stress
0.0
-6.0
0.2
homologous temperature
1.0
D
6
15
0.0
-6.0
0.2
1.0
C
6
7
8
9
10
15
D
C

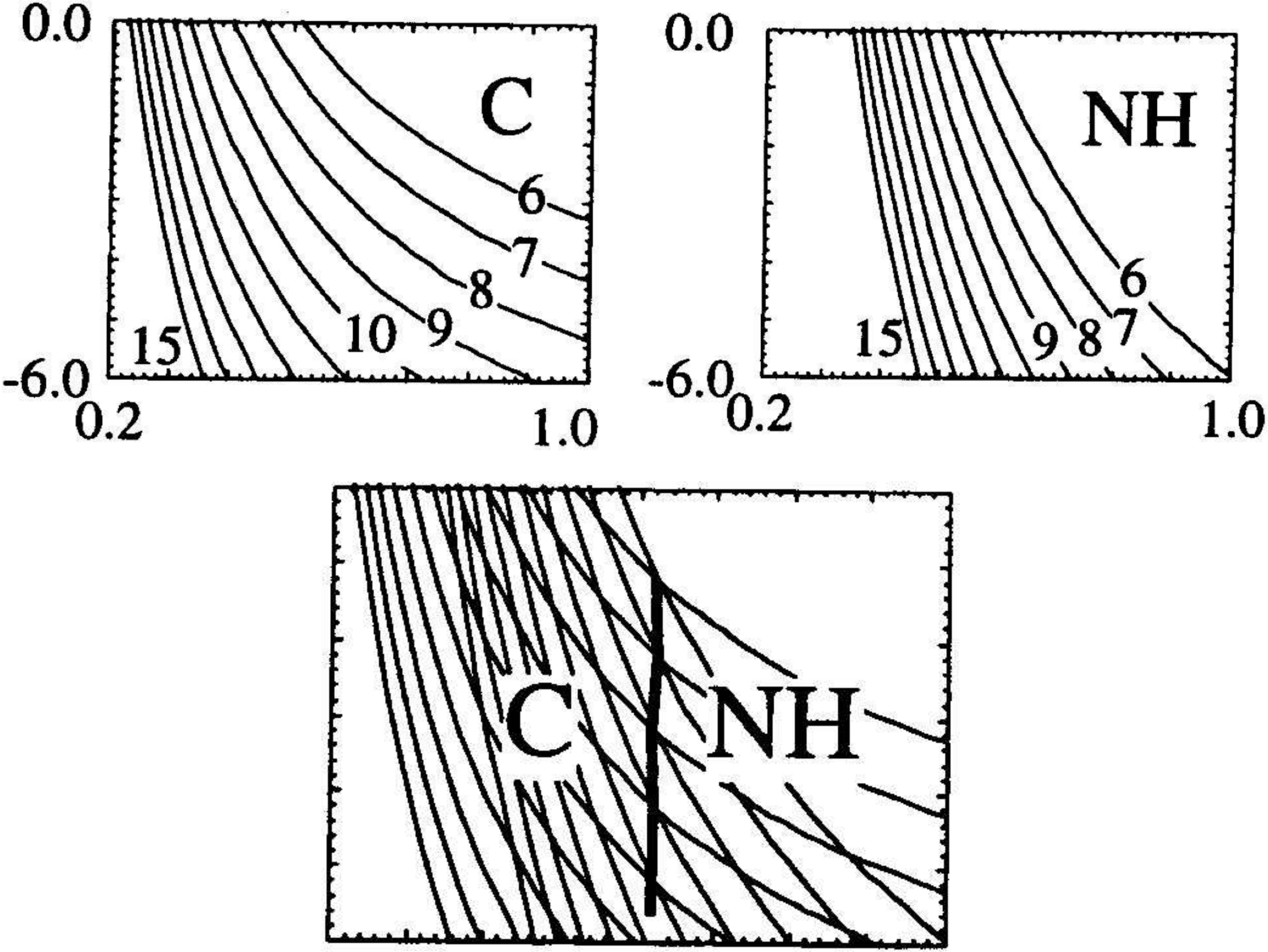
0.0
C
6
7
8
9
10
15
-6.0
0.2
1.0
0.0
NH
6
7
8
9
15
-6.0
0.2
1.0
C
NH

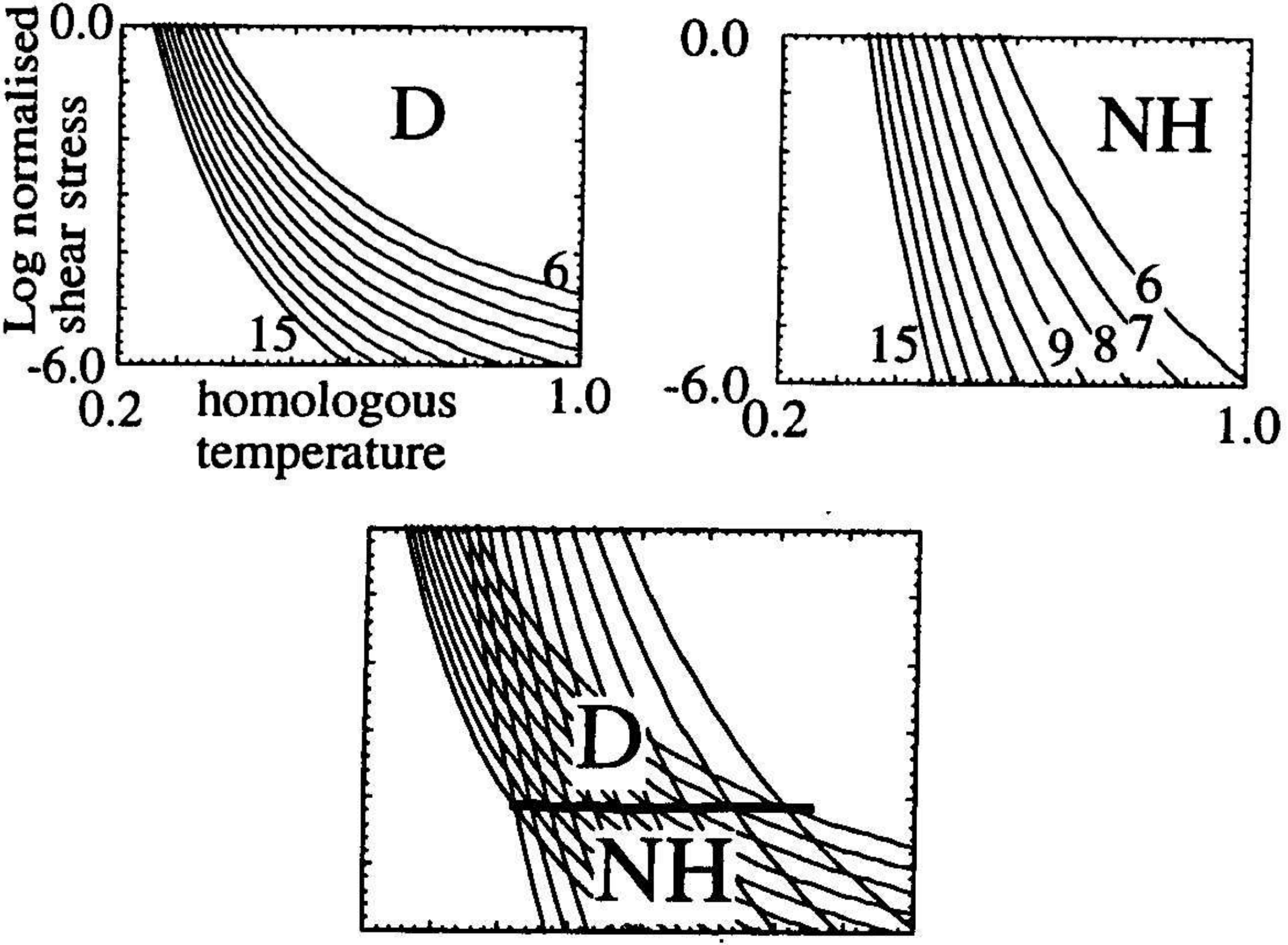
Log normalised shear stress
0.0
-6.0
0.2
1.0
homologous temperature
D
6
15
0.0
-6.0
0.2
1.0
NH
6
7
8
9
15
D
NH

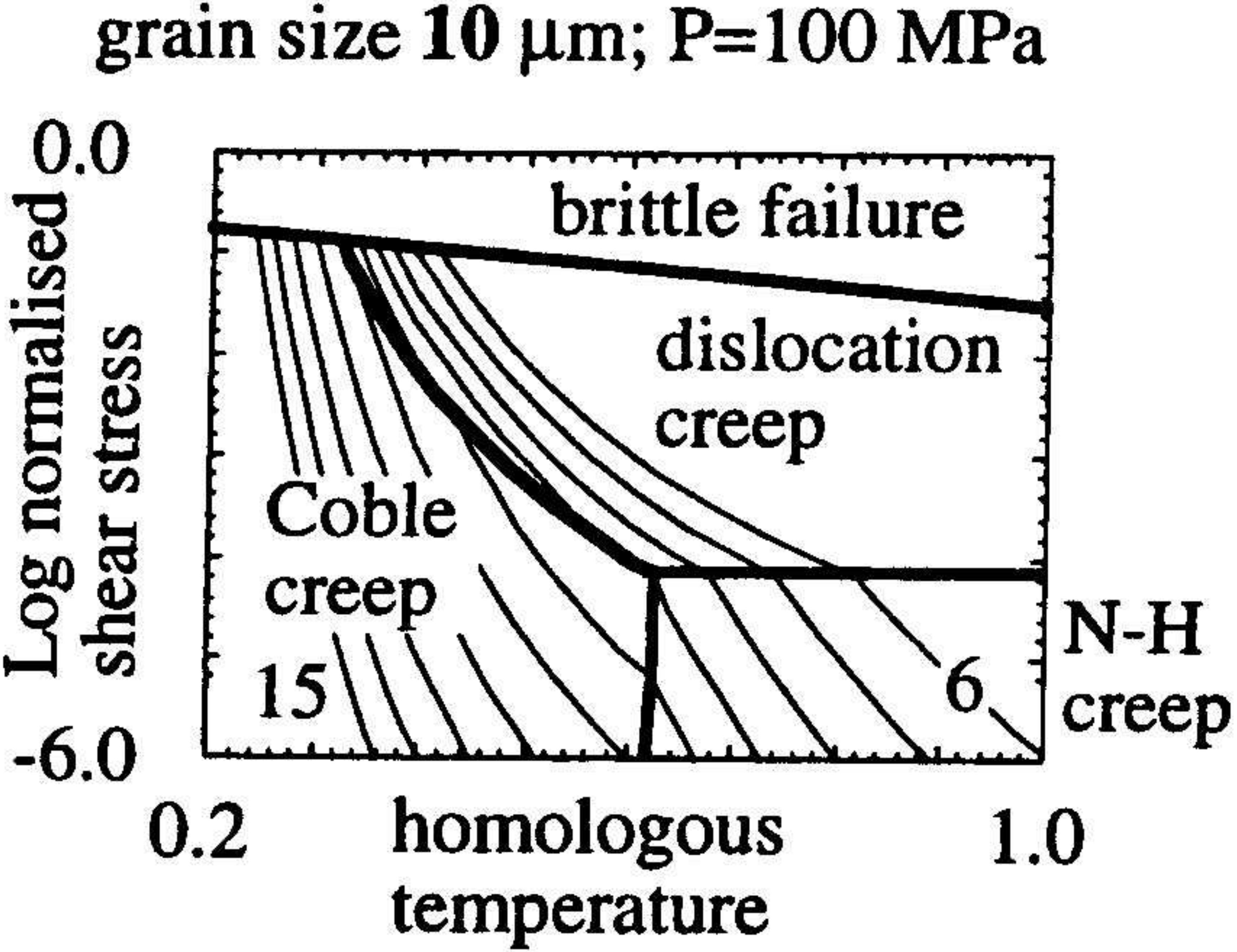
grain size **10** μm; P=100 MPa
Log normalised shear stress
0.0
-6.0
brittle failure
dislocation creep
Coble creep
15
6
N-H creep
0.2
homologous temperature
1.0

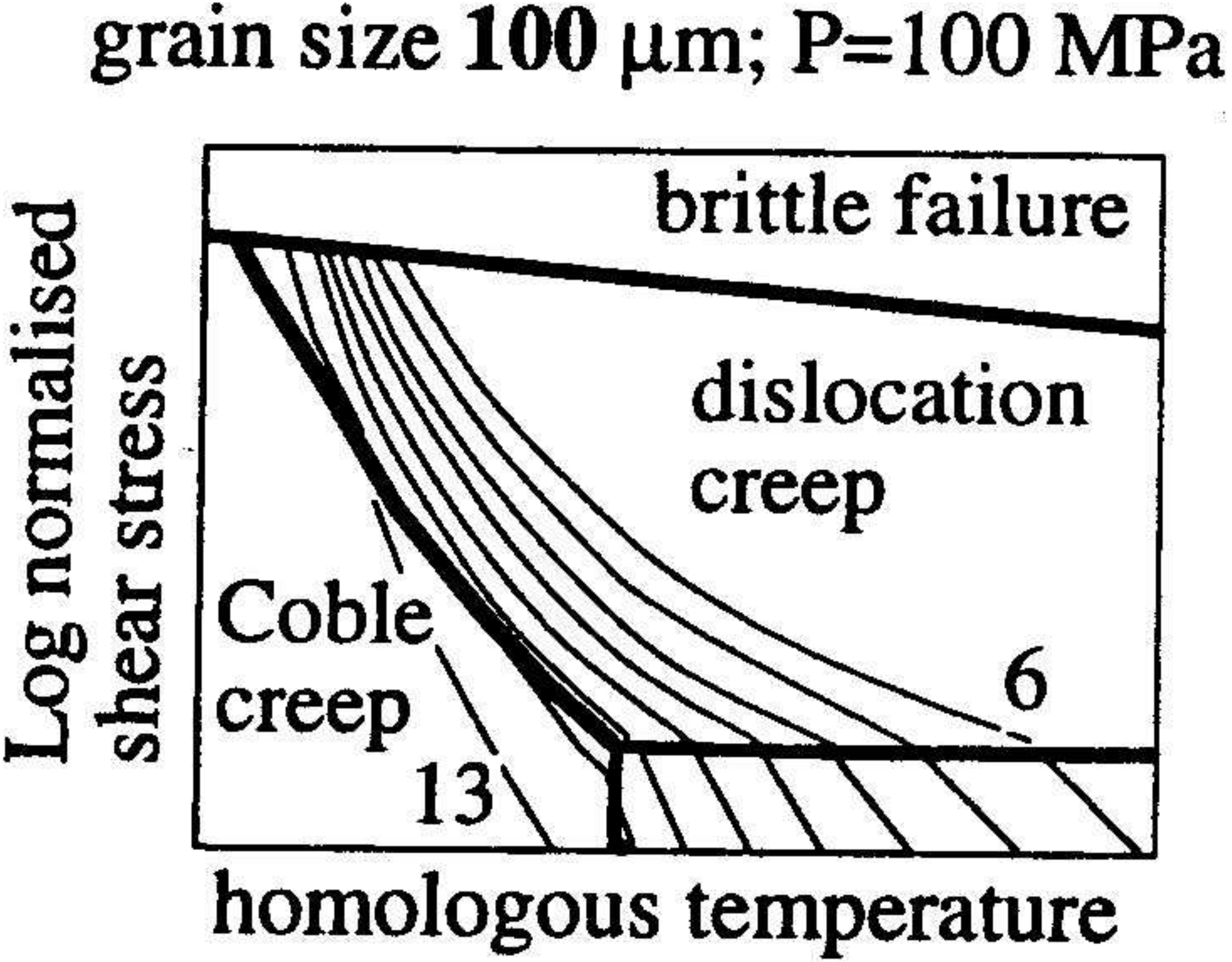
grain size **100** μm; P=100 MPa
brittle failure
dislocation creep
Coble creep
13
6
Log normalised shear stress
homologous temperature

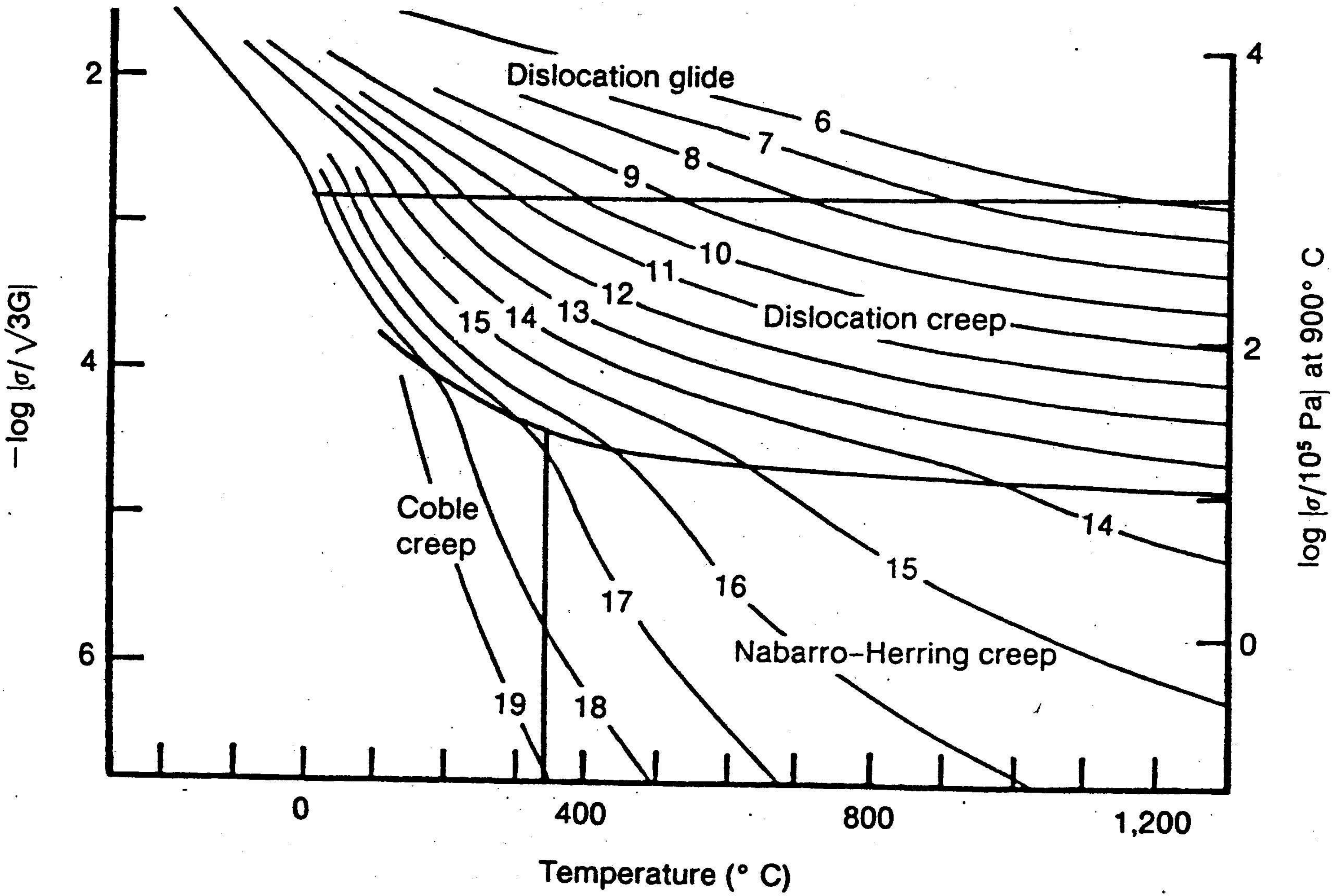
Dislocation glide
6
7
8
9
10
11
12
13
14
15
Dislocation creep
14
15
16
17
18
19
Coble creep
Nabarro–Herring creep
2
4
6
−log |σ/√3G|
4
2
0
log |σ/10⁵ Pa| at 900° C
0
400
800
1,200
Temperature (° C)

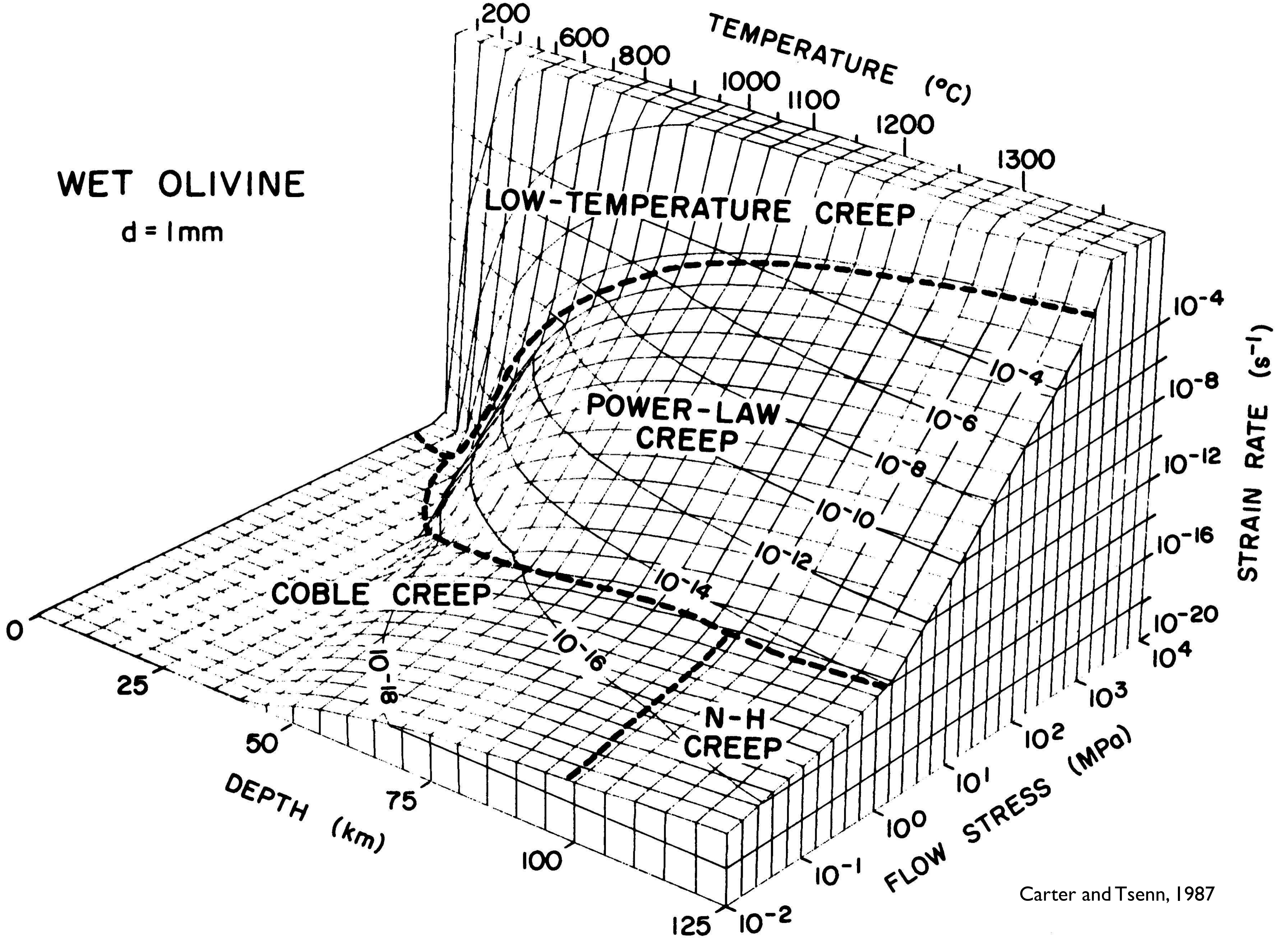

Carter and Tsenn, 1987

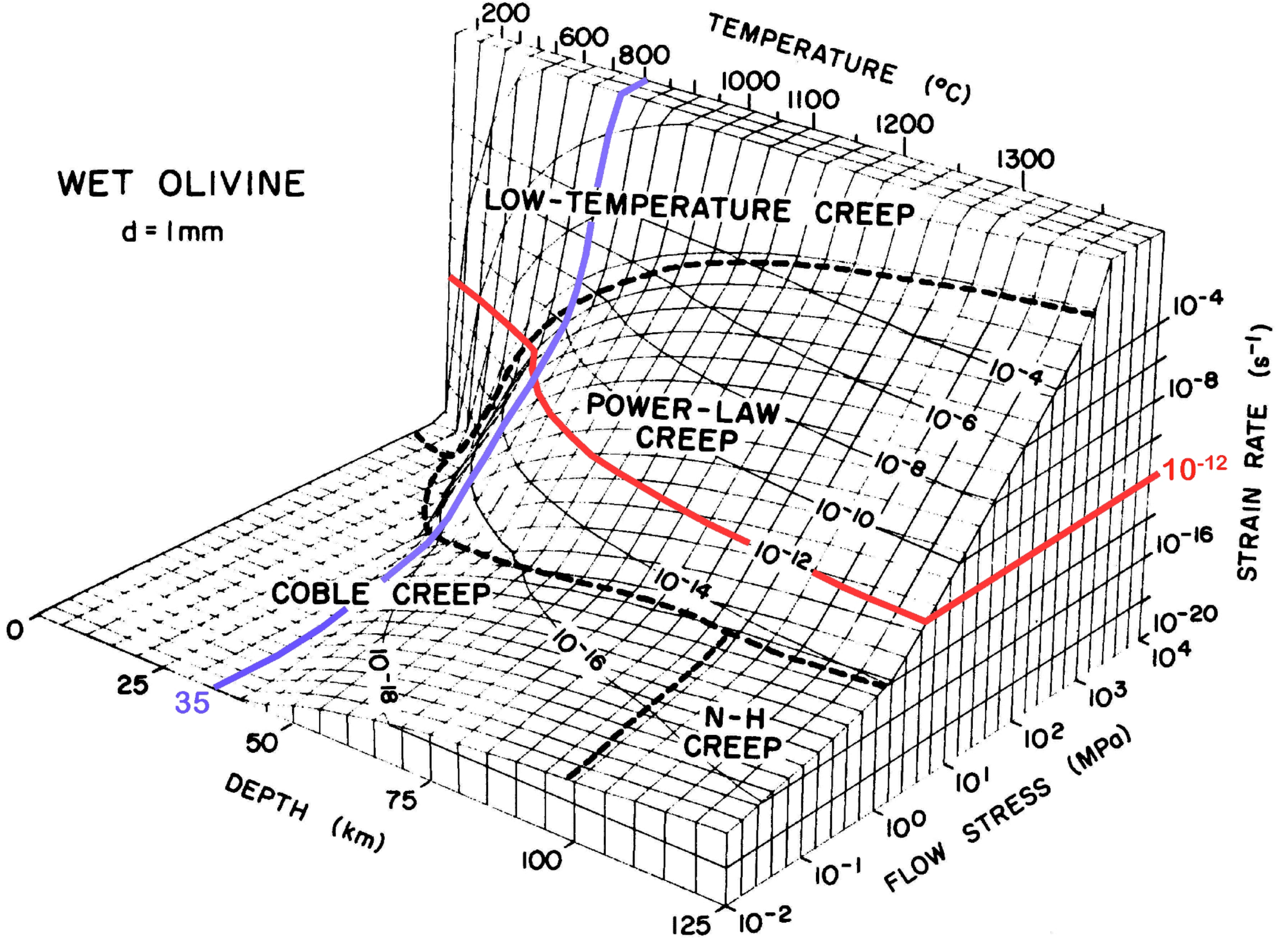
WET OLIVINE
d = 1mm
TEMPERATURE (°C)
200
600
800
1000
1100
1200
1300
LOW-TEMPERATURE CREEP
POWER-LAW CREEP
COBLE CREEP
N-H CREEP
10^-4
10^-6
10^-8
10^-10
10^-12
10^-14
10^-16
10^-18
STRAIN RATE (s^-1)
10^-4
10^-8
10^-12
10^-16
10^-20
FLOW STRESS (MPa)
10^4
10^3
10^2
10^1
10^0
10^-1
10^-2
DEPTH (km)
0
25
35
50
75
100
125

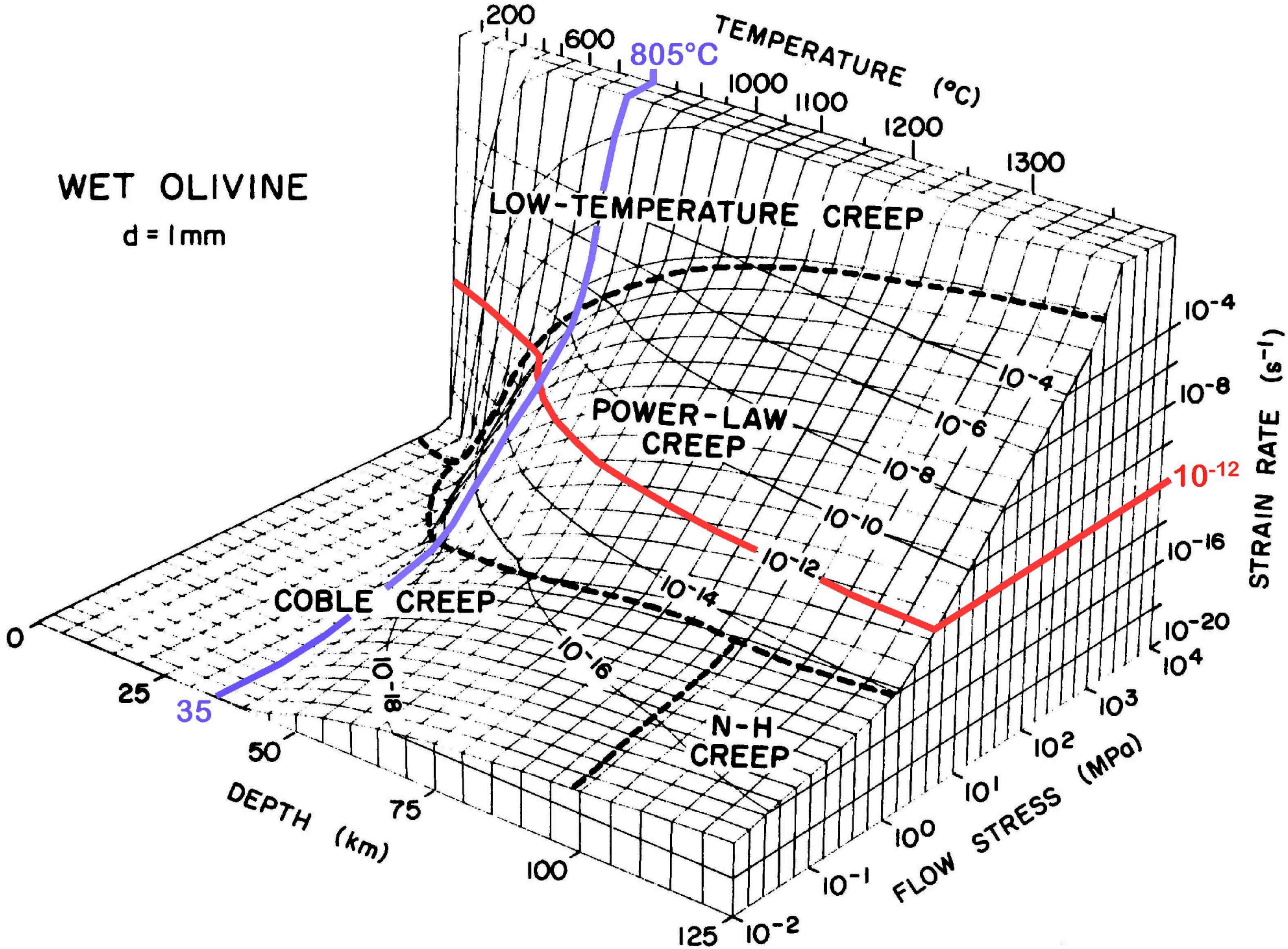
WET OLIVINE
d = 1mm
TEMPERATURE (°C)
200
600
805°C
1000
1100
1200
1300
LOW-TEMPERATURE CREEP
POWER-LAW CREEP
COBLE CREEP
N-H CREEP
10^{-4}
10^{-6}
10^{-8}
10^{-10}
10^{-12}
10^{-14}
10^{-16}
10^{-18}
STRAIN RATE (s^{-1})
10^{-4}
10^{-8}
10^{-12}
10^{-16}
10^{-20}
FLOW STRESS (MPa)
10^{4}
10^{3}
10^{2}
10^{1}
10^{0}
10^{-1}
10^{-2}
DEPTH (km)
0
25
35
50
75
100
125

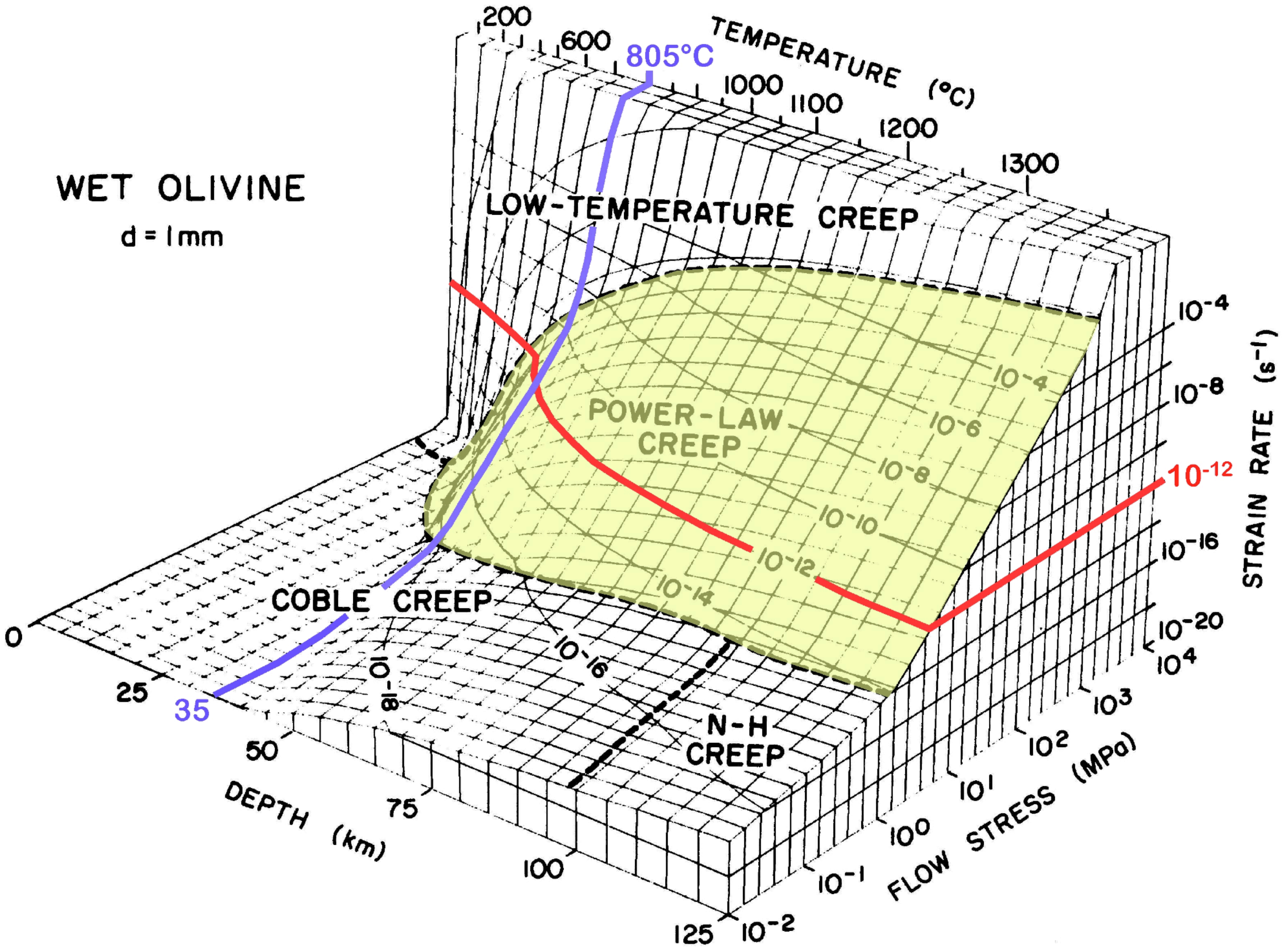
WET OLIVINE
d = 1mm
TEMPERATURE (°C)
200
600
805°C
1000
1100
1200
1300
LOW-TEMPERATURE CREEP
POWER-LAW CREEP
COBLE CREEP
N-H CREEP
10-4
10-6
10-8
10-10
10-12
10-14
10-16
10-18
STRAIN RATE (s-1)
10-4
10-8
10-12
10-16
10-20
DEPTH (km)
0
25
35
50
75
100
125
FLOW STRESS (MPa)
10-2
10-1
100
101
102
103
104

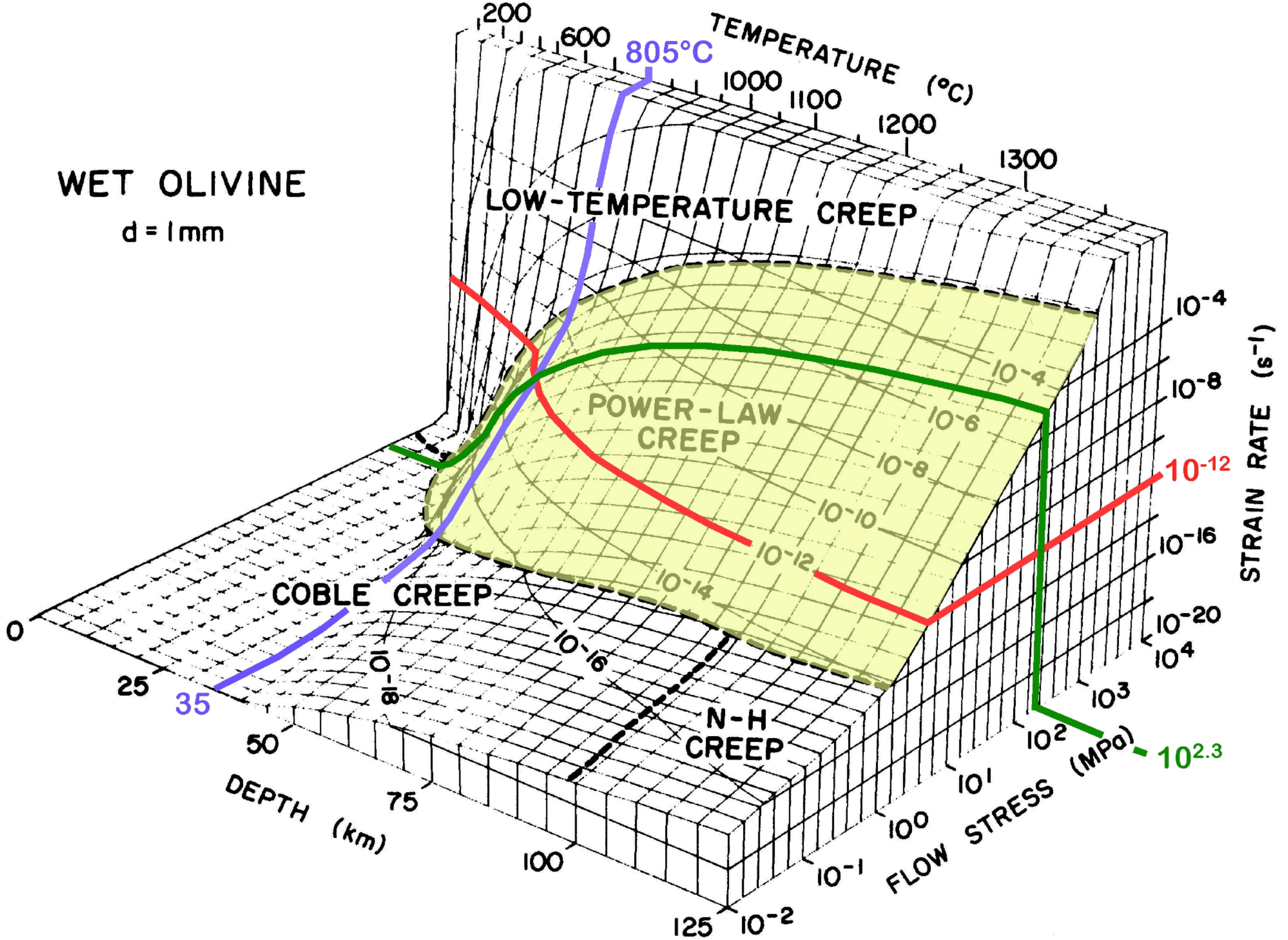
WET OLIVINE
d = 1mm
TEMPERATURE (°C)
200
600
805°C
1000
1100
1200
1300
LOW-TEMPERATURE CREEP
POWER-LAW CREEP
10^{-4}
10^{-6}
10^{-8}
10^{-10}
10^{-12}
10^{-14}
10^{-16}
10^{-18}
COBLE CREEP
N-H CREEP
STRAIN RATE (s^{-1})
10^{-4}
10^{-8}
10^{-12}
10^{-16}
10^{-20}
FLOW STRESS (MPa)
10^{4}
10^{3}
10^{2}
$10^{2.3}$
10^{1}
10^{0}
10^{-1}
10^{-2}
DEPTH (km)
0
25
35
50
75
100
125

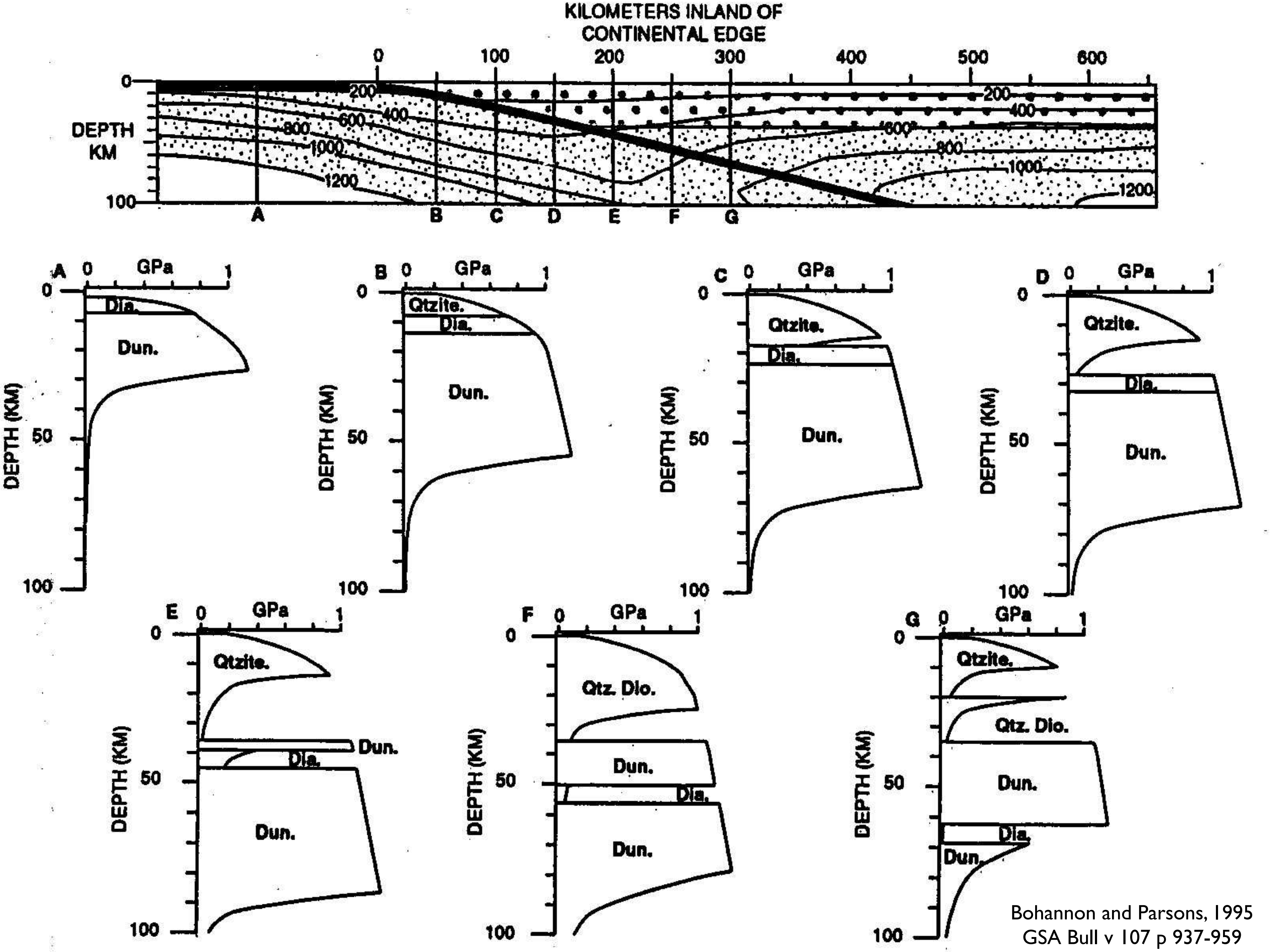

Bohannon and Parsons, 1995
GSA Bull v 107 p 937-959

“Flake” tectonics involving strong upper continental crust moving over a weaker lower continental crust (crustal asthenosphere)

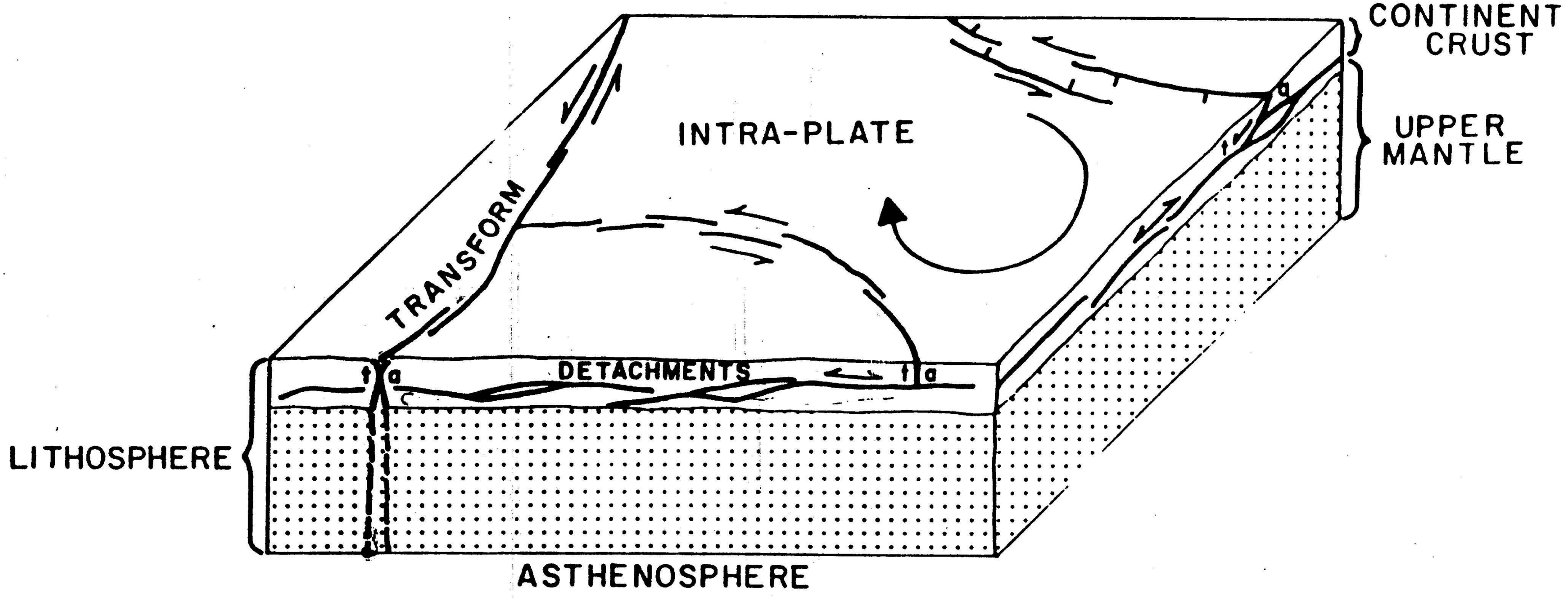

from Lemiszki and Brown